loss-of-function studies, but reproducible nonetheless. These results suggest an important role of Myc proteins in positive regulation of ICAD expression.

Finally, we examined if there might be a correlation between *ICAD* and *Myc* expression levels in cancer cell lines. The mRNA expression of *ICAD* and *c-Myc* in human oral squamous cell carcinomas (Ca22-9, HSC-2, and HSC-3), in which *ICAD* expression has not been investigated to date, as well as in Huh-7 cells during their late exponential phase of growth, was analyzed by quantitative RT-PCR (Fig. 5c). *ICAD* mRNA was readily detected in all cancer cells but the expression level was not consistent. A relatively high level of expression was observed in Ca22-9 and HSC-3 cells, while HSC-2 cells demonstrated the lowest. Interestingly, expression pattern of *c-Myc* mRNA in these cell lines showed a tendency similar to that of ICAD, suggesting an important role of Myc in ICAD expression in human cancers. A large scale analysis for investigating correlation between ICAD and Myc expression in a variety of cancer tissues obtained from patients is ongoing.

Several studies have shown up- or down-regulation of ICAD in a variety of human cancers [11–14, 29, 30]. Although transcriptional deregulation is presumably involved in this aberrant expression of ICAD, little is known about the transcriptional regulation of *ICAD* in human cells. This work was done to characterize the human *ICAD* promoter and to examine transcription factors which may be involved in its regulation. We experimentally determined putative transcription start sites by employing the 5′-RACE method, and identified a promoter region required for basal *ICAD* gene expression using promoter-reporter constructs with progressive deletions. A combined study of site-directed mutagenesis of a reporter construct and chromatin immunoprecipitation revealed the importance of an E box Myc-binding motif located at position −103 to −98 from the transcription start sites, as well as an in vivo interaction between c-Myc and N-Myc and the proximal *ICAD* promoter. Furthermore, we demonstrated the functional importance of Myc proteins with regard to transcriptional regulation of the ICAD gene from studies examining ectopic expression of c-Myc and N-Myc, as well as with RNAi technology. We showed that expression levels of ICAD and Myc correlate in some tumors.

c-Myc and N-Myc are transcription factors of the bHLH LZ family that bind to the E box sequence within promoters to control proliferation, cell differentiation, and apoptosis [25, 31, 32]. *c-myc* and *N-myc* genes are deregulated in a number of human cancers and influence proliferation and growth. A link between Myc and cancer is well established both in vivo and in vitro, and oncogenic activation of Myc has been observed to promote the development of a number of clinically significant cancers [25, 33]. However, the molecular and cellular mechanisms of Myc-mediated transformation are not fully understood. Although a variety of Myc target genes were identified and recruitment of Myc to the target promoters such as prothymosin and telomerase were shown [34], there has been no direct evidence on involvement of Myc in regulation of ICAD expression. It is known that c-Myc activation usually occurs during the later stages of carcinoma in humans. Conversely, in premalignant cells, c-Myc is a robust stimulator of apoptosis and programmed cell death [32]. One area of investigation into cancer cell death mechanisms centers on the mechanism by which c-Myc stimulates or suppresses apoptosis. For instance, Myc has been reported to potentiate apoptosis through both p53-dependent and -independent mechanisms [35, 36]. Myc controls the balance between pro- and anti-apoptotic factors at the level of the mitochondria, thereby regulating cytochrome C release and activation of downstream caspases [37, 38]. Involvement of Myc in up-regulation of ICAD expression as demonstrated in this study might present a novel mechanism of Myc-dependent inhibition of apoptosis. It is possible that elevated levels of ICAD in cells inhibit activation of endonuclear activity, thereby increasing the threshold for apoptosis signaling.

Kawane et al. have reported on the structure and analyzed the promoter of a murine *ICAD* gene, by which they demonstrated that a 118-bp flanking region of the *ICAD* gene is required for its transcription [16]. The mouse sequence shares approximately 82% homology with a corresponding upstream region of the human *ICAD* gene. The mouse *ICAD* promoter has a number of potential binding sites for transcription factors, such as Ikaros, c-Rel, Myc, and Gfi-1 [16]. Conservation of the Myc-binding motif among human and murine promoters suggests a functional significance of Myc in transcriptional regulation of *ICAD* expression.

In conclusion, this is the first report to identify a functional promoter of the human *ICAD* gene, and to demonstrate that Myc proteins are able to positively regulate ICAD gene expression. Extensive apoptosis research to date has shown that tumor aggression depends on various defects in apoptosis signaling [39]. Further investigation into the molecular events linking Myc expression with *ICAD* gene regulation may provide insight into Myc's role in cell proliferation, transformation and apoptosis.

Acknowledgements The authors gratefully acknowledge Dr. H. Kondo of Osaka University for providing the Myc-expressing plasmids. They also thank M. Matsuda, M. Ikeda, S. Yoshizaki, and T. Shimoji for their technical assistance. This work was partially supported by a grant-in-aid for Scientific Research from the Japan Society for the Promotion of Science, from the Ministry of Health, Labour and Welfare of Japan and from the Ministry of Education, Culture, Sports, Science and

Technology, and by the Program for Promotion of Fundamental Studies in Health Sciences of the National Institute of Biomedical Innovation of Japan.

References

1. Raff MC (1992) Social controls on cell survival and cell death. Nature 356:397–400. doi:10.1038/356397a0
2. Liu X, Zou H, Slaughter C, Wang X (1997) DFF, a heterodimeric protein that functions downstream of caspase-3 to trigger DNA fragmentation during apoptosis. Cell 89:175–184. doi:10.1016/S0092-8674(00)80197-X
3. Enari M, Sakahira H, Yokoyama H et al (1998) A caspase-activated DNase that degrades DNA during apoptosis, and its inhibitor ICAD. Nature 391:43–50. doi:10.1038/34112
4. Sabol SL, Li R, Lee TY, Abdul-Khalek R (1998) Inhibition of apoptosis-associated DNA fragmentation activity in nonapoptotic cells: the role of DNA fragmentation factor-45 (DFF45/ICAD). Biochem Biophys Res Commun 253:151–158. doi:10.1006/bbrc.1998.9770
5. Sakahira H, Enari M, Nagata S (1998) Cleavage of CAD inhibitor in CAD activation and DNA degradation during apoptosis. Nature 391:96–99. doi:10.1038/34214
6. Samejima K, Earnshaw WC (1998) ICAD/DFF regulator of apoptotic nuclease is nuclear. Exp Cell Res 243:453–459. doi:10.1006/excr.1998.4212
7. Nagata S (2000) Apoptotic DNA fragmentation. Exp Cell Res 256:12–18. doi:10.1006/excr.2000.4834
8. Nagata S, Nagase H, Kawane K et al (2003) Degradation of chromosomal DNA during apoptosis. Cell Death Differ 10:108–116. doi:10.1038/sj.cdd.4401161
9. Mukae N, Enari M, Sakahira H et al (1998) Molecular cloning and characterization of human caspase-activated DNase. Proc Natl Acad Sci USA 95:9123–9128. doi:10.1073/pnas.95.16.9123
10. Leek JP, Carr IM, Bell SM, Markham AF, Lench NJ (1997) Assignment of the DNA fragmentation factor gene (DFFA) to human chromosome bands 1p36.3–>p36.2 by in situ hybridization. Cytogenet Cell Genet 79:212–213
11. Charrier L, Jarry A, Toquet C et al (2002) Growth phase-dependent expression of ICAD-L/DFF45 modulates the pattern of apoptosis in human colonic cancer cells. Cancer Res 62:2169–2174
12. Abel F, Sjoberg RM, Ejeskar K, Krona C, Martinsson T (2002) Analyses of apoptotic regulators CASP9 and DFFA at 1P36.2, reveal rare allele variants in human neuroblastoma tumours. Br J Cancer 86:596–604. doi:10.1038/sj.bjc.6600111
13. Konishi S, Ishiguro H, Shibata Y et al (2002) Decreased expression of DFF45/ICAD is correlated with a poor prognosis in patients with esophageal carcinoma. Cancer 95:2473–2478. doi:10.1002/cncr.10987
14. Brustmann H (2006) DNA fragmentation factor (DFF45): expression and prognostic value in serous ovarian cancer. Pathol Res Pract 202:713–720. doi:10.1016/j.prp.2006.06.003
15. Sacco R, Tsutsumi T, Suzuki R et al (2003) Antiapoptotic regulation by hepatitis C virus core protein through up-regulation of inhibitor of caspase-activated DNase. Virology 317:24–35. doi:10.1016/j.virol.2003.08.028
16. Kawane K, Fukuyama H, Adachi M et al (1999) Structure and promoter analysis of murine CAD and ICAD genes. Cell Death Differ 6:745–752. doi:10.1038/sj.cdd.4400547
17. Masaki T, Matsuura T, Ohkawa K et al (2006) All-trans retinoic acid down-regulates human albumin gene expression through the induction of C/EBPbeta-LIP. Biochem J 397:345–353. doi:10.1042/BJ20051863
18. Suzuki Y, Yamashita R, Sugano S, Nakai K (2004) DBTSS, DataBase of Transcriptional Start Sites: progress report 2004. Nucleic Acids Res 32:D78–D81. doi:10.1093/nar/gkh076
19. Wingender E, Dietze P, Karas H, Knuppel R (1996) TRANSFAC: a database on transcription factors and their DNA binding sites. Nucleic Acids Res 24:238–241. doi:10.1093/nar/24.1.238
20. Bello-Fernandez C, Packham G, Cleveland JL (1993) The ornithine decarboxylase gene is a transcriptional target of c-Myc. Proc Natl Acad Sci USA 90:7804–7808. doi:10.1073/pnas.90.16.7804
21. Meier JL, Luo X, Sawadogo M, Straus SE (1994) The cellular transcription factor USF cooperates with varicella-zoster virus immediate-early protein 62 to symmetrically activate a bidirectional viral promoter. Mol Cell Biol 14:6896–6906
22. Kiermaier A, Gawn JM, Desbarats L et al (1999) DNA binding of USF is required for specific E-box dependent gene activation in vivo. Oncogene 18:7200–7211. doi:10.1038/sj.onc.1203166
23. Luscher B, Larsson LG (1999) The basic region/helix-loop-helix/leucine zipper domain of Myc proto-oncoproteins: function and regulation. Oncogene 18:2955–2966. doi:10.1038/sj.onc.1202750
24. Grandori C, Cowley SM, James LP, Eisenman RN (2000) The Myc/Max/Mad network and the transcriptional control of cell behavior. Annu Rev Cell Dev Biol 16:653–699. doi:10.1146/annurev.cellbio.16.1.653
25. Adhikary S, Eilers M (2005) Transcriptional regulation and transformation by Myc proteins. Nat Rev Mol Cell Biol 6:635–645. doi:10.1038/nrm1703
26. Wagner AJ, Le Beau MM, Diaz M, OHay N (1992) Expression, regulation, and chromosomal localization of the Max gene. Proc Natl Acad Sci USA 89:3111–3115. doi:10.1073/pnas.89.7.3111
27. Skouteris GG, Schroder CH (1996) c-Myc and Max interactions in quiescent and mitogen-stimulated primary hepatocytes. Exp Cell Res 225:237–244. doi:10.1006/excr.1996.0173
28. Kato H, Okamura K, Kurosawa Y et al (1989) Characterization of DNA rearrangements of N-Myc gene amplification in three neuroblastoma cell lines by pulsed-field gel electrophoresis. FEBS Lett 250:529–535. doi:10.1016/0014-5793(89)80790-2
29. Masuoka J, Shiraishi T, Ichinose M, Mineta T, Tabuchi K (2001) Expression of ICAD-l and ICAD-S in human brain tumor and its cleavage upon activation of apoptosis by anti-Fas antibody. Jpn J Cancer Res 92:806–812
30. Yang HW, Chen YZ, Piao HY et al (2001) DNA fragmentation factor 45 (DFF45) gene at 1p36.2 is homozygously deleted and encodes variant transcripts in neuroblastoma cell line. Neoplasia 3:165–169. doi:10.1038/sj.neo.7900141
31. Secombe J, Pierce SB, Eisenman RN (2004) Myc: a weapon of mass destruction. Cell 117:153–156. doi:10.1016/S0092-8674(04)00336-8
32. Meyer N, Kim SS, Penn LZ (2006) The Oscar-worthy role of Myc in apoptosis. Semin Cancer Biol 16:275–287. doi:10.1016/j.semcancer.2006.07.011
33. Donaldson TD, Duronio RJ (2004) Cancer cell biology: Myc wins the competition. Curr Biol 14:R425–R427
34. Mac SM, D'Cunha CA, Farnham PJ (2000) Direct recruitment of N-Myc to target gene promoters. Mol Carcinog 29:76–86
35. Sakamuro D, Eviner V, Elliott KJ et al (1995) c-Myc induces apoptosis in epithelial cells by both p53-dependent and p53-independent mechanisms. Oncogene 11:2411–2418

36. Nilsson JA, Cleveland JL (2003) Myc pathways provoking cell suicide and cancer. Oncogene 22:9007–9021
37. Juin P, Hueber AO, Littlewood T, Evan G (1999) c-Myc-induced sensitization to apoptosis is mediated through cytochrome c release. Genes Dev 13:1367–1381
38. Hotti A, Jarvinen K, Siivola P, Holtta E (2000) Caspases and mitochondria in c-Myc-induced apoptosis: identification of ATM as a new target of caspases. Oncogene 19:2354–2362
39. Hanahan D, Weinberg RA (2000) The hallmarks of cancer. Cell 100:57–70

JOURNAL OF VIROLOGY, July 2008, p. 6942–6951
0022-538X/08/$08.00+0 doi:10.1128/JVI.00662-08

Vol. 82, No. 14

Identification of Mutated Cyclization Sequences That Permit Efficient Replication of West Nile Virus Genomes: Use in Safer Propagation of a Novel Vaccine Candidate▽

Ryosuke Suzuki,[1,3] Rafik Fayzulin,[1] Ilya Frolov,[2] and Peter W. Mason[1,2]*

Department of Pathology[1] and Department of Microbiology and Immunology,[2] University of Texas Medical Branch, Galveston, Texas 77555, and Department of Virology II, National Institute of Infectious Diseases, Shinjuku-ku, Tokyo, 162-8640, Japan[3]

Received 25 March 2008/Accepted 28 April 2008

Existing live-attenuated flavivirus vaccines (LAV) could be improved by reducing their potential to recombine with naturally circulating viruses in the field. Since the highly conserved cyclization sequences (CS) found in the termini of flavivirus genomes must be complementary to each other to support genome replication, we set out to identify paired mutant CS that could support the efficient replication of LAV but would be unable to support replication in recombinant viruses harboring one wild-type (WT) CS. By systematic evaluation of paired mutated CS encoded in West Nile virus (WNV) replicons, we identified variants having single and double mutations in the 5′- and 3′-CS components that could support genome replication at WT levels. Replicons containing only the double-mutated CS in the 5′ or the 3′ ends of the genome were incapable of replication, indicating that mutated CS could be useful for constructing safer LAV. Despite the identity of the central portion of the CS in all mosquito-borne flaviviruses, viruses carrying complementary the double mutations in both the 5′- and the 3′-CS were indistinguishable from WT WNV in their replication in insect and mammalian cell lines. In addition to the utility of our novel CS pair in constructing safer LAV, we demonstrated that introduction of these mutated CS into one component of a recently described two-component genome system (A. V. Shustov, P. W. Mason, and I. Frolov, J. Virol. 81:11737-11748, 2007) enabled us to engineer a safer single-cycle WNV vaccine candidate with reduced potential for recombination during its propagation.

West Nile virus (WNV) is a member of the genus *Flavivirus* of the family *Flaviviridae*, a genus that includes dengue virus (DENV), Japanese encephalitis virus (JEV), yellow fever virus (YFV), and tick-borne encephalitis virus (12). The diseases caused by these viruses have a serious impact on public health, especially in developing countries. WNV has spread widely in the United States since its introduction in 1999 and become a major public health problem, producing significant morbidity and mortality (42).

WNV, like other flaviviruses, is an enveloped, positive-strand RNA virus with a genome of about 11 kb. A single open reading frame encodes the viral polyprotein, which is processed co- and posttranslationally into the structural (C, prM/M, and E) and nonstructural (NS1, NS2A, NS2B, NS3, NS4A, NS4B, and NS5) proteins. This open reading frame is flanked by 5′ and 3′ untranslated regions (UTRs). The viral structural proteins form infectious viral particles. The nonstructural proteins responsible for various enzymatic activities, including those of the RNA-dependent RNA polymerase, helicase, and protease, are all essential for viral genome replication (24). Furthermore, the NS proteins also are capable of interfering with some aspects of the infected cell's innate immune responses to infection (6, 23, 26, 31, 32), and some NS proteins have also been shown to be required for efficient virion assembly (22, 25).

Early studies on mosquito-borne flaviviruses identified highly conserved short complementary sequences near the 5′ and 3′ ends of flavivirus genomes that included an eight-nucleotide core sequence that is conserved among all mosquito-borne flaviviruses. These sequences were predicted to circularize the genome (17) and have therefore been termed cyclization sequences (CS). The 5′ CS is located within the C coding region, and the 3′ CS is present in the 3′ UTR, just upstream of a 3′-terminal stem-loop structure that is also highly conserved among all flaviviruses (11, 43) and is thought to function as a critical element of the promoter for minus-strand-RNA synthesis (10). Recently it was reported that another RNA interaction between a region upstream of the viral AUG (defined as the upstream AUG region, or 5′ UAR) and a complementary 3′ UAR found at the end of the viral genome are required for efficient replication of DENV2 (3) and WNV (45) genomes.

Several studies on CS have shown that their complementarity, rather than nucleotide sequence, is a prerequisite for replication of the genomes of WNV, YFV, and DENV (1, 2, 13, 19, 27). However, the precise nucleotide sequence of CS also appear to be important for efficient viral RNA replication, since genomes with unnatural CS, although viable, usually replicate more poorly than wild-type (WT) genomes (2, 19, 27).

Live-attenuated vaccines (LAV) for yellow fever and Japanese encephalitis are in widespread use, and LAV for other

* Corresponding author. Mailing address: The University of Texas Medical Branch, 301 University Boulevard, Galveston, TX 77555-0436. Phone: (409) 747-8143. Fax: (409) 747-8150. E-mail: pwmason@utmb.edu.

▽ Published ahead of print on 14 May 2008.

flavivirus diseases, including dengue and West Nile encephalitis, are in different stages of development (7, 8, 16, 18, 21, 29, 34, 35, 40). LAV offer considerable advantage over inactivated viral vaccines or subunit vaccines in terms of efficacy and cost. However, there is a concern that recombination between these LAV and naturally circulated flaviviruses could result in generation of unnatural viruses with increased virulence over either natural or vaccine strains (38). This potential problem can be addressed by engineering unnatural CS in the LAV genomes such that their 5′ and 3′ CS are not complementary to the corresponding CS elements of circulating WT viruses. Thus, recombinant genomes generated by a single round of recombination between these LAV genomes and WT genetic material would not be viable. Recently, we showed that flaviviruses can replicate as two-component genome viruses, a system that opens up the opportunity of producing a new class of LAV (39). However, large-scale production of these viruses in vitro requires coinfection of two defective genomes in the same cell, providing a situation that could result in intergenomic recombination leading to the production of replication-competent viruses that could be pathogenic. Thus, the safety of this two-component system would be enhanced by the introduction of mutated CS into one of the two defective genomes. However, to be efficiently utilized for both enhancing LAV safety and improving our two-component genome system, there is a need for mutated CS that support highly efficient genome replication.

In this study, a large number of nucleotide substitutions were systematically introduced into the CS in both the 5′ and 3′ regions of a WNV subgenomic replicon (WNR), and the mutated genomes were tested for their replication efficiency. Using this strategy, we selected mutations in the 5′ and 3′ CS elements that supported efficient replication of WNV genomes and allowed them to be packaged into infectious particles. Two such mutations were combined (to increase their genetic stability) and further investigated to demonstrate that genomes with these mutations only in the 5′ CS or only in the 3′ CS were unable to replicate. These results suggest that the mutated CS could be useful for development of safer LAV with reduced probability of generating recombinant viruses with naturally circulating flaviviruses. Surprisingly, the replication of viruses engineered to contain these double-mutant CS in both mammalian and insect cells was indistinguishable from that of WT virus. Furthermore, we inserted these mutations into one component of our previously described two-component genome vaccine (39) and showed that a genome containing matched WT CS could efficiently complement a genome containing the matched mutant CS, producing high titers of infectious particles. These data demonstrate the utility of CS mutations in generating two-component genome vaccines with a reduced capacity to generate viable virus in the event of single-round recombination with only one crossover.

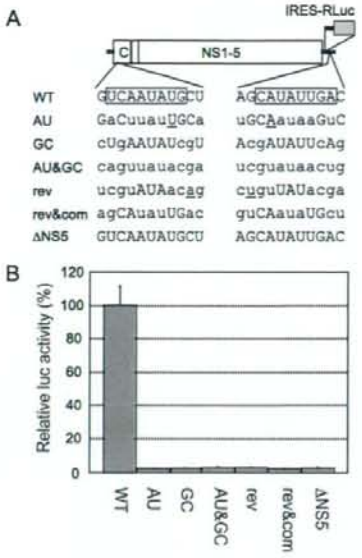

FIG. 1. Effects of nucleotide sequence of CS on RNA replication. (A) Schematic representation of WNV replicon RNA structure (WNR-CNS1-5Rluc) and position of the Rluc-encoding cistron. The nucleotide sequences of CS are indicated next to their names (see the text). Boxes indicate the eight nucleotides that are 100% conserved among all mosquito-borne flaviviruses. Nucleotide substitutions in the 5′ CS and 3′ CS are in lower case. Underlined nucleotides were exceptions to the rules used to swap codons (see the text) that were implemented to avoid generation of stop codons in 5′ CS that reside in the C coding region. ΔNS5 contains WT CS and a frameshift mutation upstream of the active-site GDD motif of the RNA-dependent RNA polymerase of NS5. (B) RNA replication of WT and mutant replicons in BHK cells. BHK cells were transfected with identical amounts of in vitro-transcribed Rluc-expressing WNR RNAs. Rluc activities were measured at 5 h and 2 days posttransfection. The Rluc activity obtained at 2 days is shown normalized to activity obtained at 5 h to account for slight differences in transfection efficiency (see the text). Data for each condition are averages of triplicate values with error bars showing standard deviations; the WT control value was set to 100%. The experiment was repeated at least twice, with consistent results.

MATERIALS AND METHODS

Cells, plasmids, and viruses. BHK cells were maintained at 37°C in minimal essential medium (MEM) supplemented with 10% fetal bovine serum (FBS) and antibiotics. Vero cells were maintained at 37°C in MEM containing 6% FBS and antibiotics. BHK(VEErep/C*-E/Pac) packaging cells expressing the WNV C-prM-E proteins were propagated at 37°C in Dulbecco's MEM supplemented with 10% FBS and 10 μg/ml puromycin as previously described (14, 44). C7/10 mosquito cells were maintained at 30°C in Leibovitz's L15 medium supplemented with 10% FBS, 10% tryptose phosphate broth, and antibiotics.

A WNR genome containing the entire WNV C gene (WNR-CNS1-5) was described previously (9). WNR-CNS1-5Rluc was constructed from WNR-CNS1-5 by inserting an IRES (internal ribosome entry site)-driven humanized *Renilla* luciferase (Rluc) gene into an NsiI site located 39 bases downstream of the termination codon (see Fig. 1).

For studies requiring a full-length WNV cDNA, a previously described WNV cDNA derived from a human WNV isolate obtained in Texas in 2002 (36) was introduced into a bacterial artificial chromosome (BAC) plasmid to enhance its stability (41). A BAC-propagated cDNA derivative of our previously described single-cycle WNV lacking a functional C gene (28), designated RepliVAX WN.2, has been described (44). For the construction of the helper genome for our two-component genome system, we inserted a cassette consisting of the gene for the foot-and-mouth disease virus (FMDV)-2A autoproteinase and a codon-optimized WNV C gene between the truncated C and NS1 coding sequences in WNR-CNS1-5.

CS mutations were introduced into the cDNAs encoding the WNV (and WNR) genomes by using PCR and confirmed by sequencing. The genome sequences used in this study are available from the authors upon request.

RNA synthesis using in vitro transcription reactions. Plasmids were prepared for runoff transcription by digestion with SwaI, and the resulting template DNAs

were in vitro transcribed using a MegaScript T7 synthesis kit (Ambion) supplemented with a 7mG(ppp)G cap analogue (New England Biolabs). The yield and integrity of transcripts were analyzed by gel electrophoresis under nondenaturing conditions, and aliquots of transcription reaction products were used for transfection without additional purification.

RNA transfection. RNA was transfected into BHK monolayers using Lipofectin (Invitrogen) by a slight modification of the manufacturer's suggested protocol. Three hours after transfection, the media containing the RNA and Lipofectin mixture were removed from the cell layer, and the cells were refed with growth medium and incubated at 37°C until assayed as described below. To produce infectious WNV genome-containing particles, BHK cells and BHK packaging cells expressing WNV structural protein, BHK(VEErep/C*-E/Pac) (see above), were electroporated by T7 transcription reactions (36), and virus or virus-like particles (VLPs) containing the WNR were collected as previously described (14).

Analysis of VLPs, RepliVAX, and virus replication. Cell monolayers prepared in multiwell plates were incubated with dilutions of virus, VLPs, or RepliVAX and helper particles (two-component system) and then overlaid with medium containing 1% FBS (in some cases containing 0.8% carboxymethyl cellulose). Following incubation for the appropriate time at the appropriate temperature (see the figure legends), the monolayers were fixed and immunostained as described previously (36), and foci (or individual cells) were counted and used to calculate a titer of focus-forming units/ml for spreading infections or infectious units/ml for nonspreading infections. For most studies, infected cells were immunostained with a polyclonal anti-WNV hyperimmune ascitic fluid, but in cases where the packaging cells (which expressed WNV structural proteins) were utilized, cells containing replicating WNV genomes were stained with a monoclonal antibody to NS1 (20) (provided by E. Konishi, Kobe University). In other cases, where assay cells infected with E-expressing RepliVAX genomes needed to be distinguished from cells infected with VLPs expressing "helper" genomes (see Results), a monoclonal antibody to E (7H2; Bioreliance) was utilized. For growth curves, BHK, Vero, or C7/10 cell monolayers were infected at defined multiplicities of infection (MOIs) (see the figure legends) and then incubated at the appropriate temperature. Media were removed (and replaced with fresh media) at the indicated time points and stored at −80°C for subsequent titration as described above.

***Renilla* luciferase assay.** Monolayers of BHK cells transfected with Rluc-expressing RNAs by using Lipofectin were lysed by the addition of reporter lysis buffer (Promega), and the lysates were stored at −20°C for subsequent assays. Prior to the assays, the extracts were thawed and clarified to remove insoluble debris, and a portion of each extract was mixed with 5 volumes of an Rluc reaction buffer (100 mM EDTA, 50 mM Tris [pH 8.0] containing 5 μg/ml coelenterazine; Nanolight Technology) in black-walled 96-well microtitration plates. Following a 1-min incubation period, luminescence was determined with a Microplate luminometer (Applied Biosystems).

RNA secondary-structure prediction. RNA secondary structure and the value of ΔG were predicted by using Mfold version 3.2 (46). In cases where multiple structures were predicted, the structure with lowest free energy of initial ΔG was chosen for presentation.

RESULTS

Drastic alteration of CS abolishes RNA replication. Previous studies demonstrated that CS need to be complementary to support genome replication of flaviviruses and that their complementarity, rather than nucleotide sequence, is a prerequisite for flavivirus RNA replication (2, 19, 27). However, those studies also showed that viral genome with complementary but "unnatural" CS replicated more poorly than genomes with WT CS. In those studies, introduction of unnatural CS resulted in changes in the overall free energy of the expected interactions between the 5′ CS and 3′ CS of the tested genomes. Therefore, these altered free energies of the interaction of CS as well as the alteration of specific nucleotides could have affected RNA replication efficiency and thus could have been responsible for the observed defects in replication of the mutant CS-bearing genomes.

In our initial attempts to generate CS mutants that could not productively recombine with WT sequences, we created a series of CS mutant WNRs designed to contain substantially altered CS with multiple base changes but predicted free energies of interaction identical to the those of WT CS (Fig. 1A). To this end, all CS mutations were designed to conserve the base pairing of the 11-nucleotide 5′- and 3′-CS regions as well as the overall number of A-U and G-C base pairs to ensure that mutant genomes maintained the free energy of WT WNV. These mutant constructions include a switch of all A-U pairs to U-A, a switch of all G-C pairs to C-G, a switch of both A-U and G-C pairs, reverse sequences, and reverse and complementary sequences. Certain changes required by these "swap" algorithms were not implemented, since they would have resulted in nonviable-stop-codon generation in the 5′ CS that resides in the C coding region. In these cases, either WT nucleotides or other suitable substitutions were placed at these positions (Fig. 1A).

These mutations were incorporated into plasmids carrying Rluc-expressing WNR cDNAs (WNR-CNS1-5Rluc), and RNAs derived from these plasmids were generated in vitro and transfected into BHK cells. The Rluc activities were measured at 5 h posttransfection, providing a measurement of translation of transfected RNA, and at 48 h posttransfection, providing a measurement of RNA replication (27). The values obtained 5 h after transfection were nearly identical for all replicons, including ΔNS5, which contains a frameshift mutation upstream of the GDD motif of NS5 for a negative control with no replication activity, indicating that the CS mutations had no effect on the initial translational activity of the reporter gene encoded by the transfected replicon RNA. To facilitate analyses of replication levels, these 5-h data were used to normalize for slight differences in transfection efficiency (5-h Rluc data were usually within 50% of each other within experiments, and these 5-h values were always less than 7% of the 48 h value in the case of WT CS replicons [WNR-CNS1-5Rluc]). As shown in Fig. 1B, all five replicons harboring the CS mutations showed levels of normalized Rluc activity indistinguishable from the Rluc activity of the replication-deficient control RNA (ΔNS5). These data indicated that many possible complementary, unnatural CS with an overall free energy of hybridization similar to that of WT sequences were incapable of supporting RNA replication, demonstrating that the precise sequences of these regions are as important for replicational activity as complementarity per se.

Effects of single-nucleotide substitution within the CS on RNA replication. Following this demonstration that the large changes in CS examined in Fig. 1 were nonviable, despite their maintenance of WT free energies, we undertook a more systematic analysis of the CS. To this end, complementary single-nucleotide substitutions were introduced into CS in both 5′- and 3′-CS regions of WNR, as shown in Fig. 2A.

The Rluc activity from mutated replicons was compared with that of WT replicon RNA (WNR-CNS1-5Rluc). As shown in Fig. 2B, m1 and m2, which contain 1-bp substitutions at the terminal end of the paired CS, showed a drastic reduction of RNA replication. However, m4 and m7 displayed no detectable reduction in RNA replication. Other mutants showed moderately reduced replication efficiency (20 to 80% of WT efficiency). These data suggest that there are both critical and noncritical nucleotides in the CS. Using Mfold to produce structures from an artificial sequence created by fus-

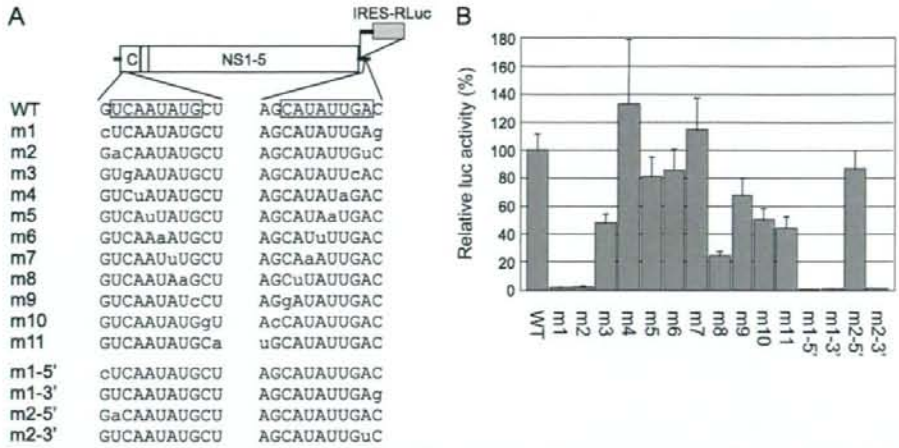

FIG. 2. Effect of single nucleotide mutations in CS on WNV RNA replication. (A) Schematic representation of WNR RNA structure. The nucleotide sequences of mutant CS are indicated next to their respective names. Boxes indicate the eight nucleotides that are 100% conserved among all mosquito-borne flaviviruses. Nucleotide substitutions in the 5′ CS and 3′ CS are in lower case. (B) RNA replication of WT and mutant replicons in BHK cells. Averages of triplicate relative luciferase activities at 2 days posttransfection were normalized to that at 5 h, and the WT control value was set to 100%; error bars show standard deviations. The experiment was repeated at least twice, producing similar results.

ing 52 bases of the C coding region, 31 bases of the 3′ UTR, and a 38-nucleotide A stuffer, we were able to show that the predicted structures of all mutants were indistinguishable from those of the parental CS (data not shown). Thus, it appears that these apparent site-specific nucleotide requirements were likely not due to a large alteration of secondary structures predicted for this region.

To help determine if these site-specific requirements reflected sequence-specific needs in only one CS or the other, we examined the replication-incompetent m1 and m2 mutants in more detail. To this end, we constructed reporter RNA replicons containing the m1 or m2 mutation in only the 5′ UTR or 3′ UTR (Fig. 2A). As shown in Fig. 2B, m1-5′, m1-3′, and m2-3′ showed drastically reduced replication of RNA, whereas m2-5′ showed only slight reduction of RNA replication compared to the WT (WNR-CNS1-5Rluc). Surprisingly, m2-5′ could replicate much better than m2, which altered both the 5′ CS position (U to A) and 3′ CS position (A to U), suggesting that A at position 2 in 3′ CS, rather than base pairing, is critical for efficient RNA replication. In contrast, the nucleotide at position 1 in CS appeared to be critical in both the 5′ UTR and 3′ UTR, although we could not exclude the possibility that base pairing per se was critical at this residue.

Effect of combined CS mutations on RNA replication and viral genome packaging. To help produce an altered CS that would be unlikely to be able to support replication when combined with a WT sequence, we decided to create a CS with two separate mutations. To this end, we combined the two mutations (m4 and m7) that appeared to support WT levels of replication with each other, creating CS with a combination of these substitutions (m4/7; Fig. 3A). Transcribed RNA encoding this double mutant was introduced into BHK, and Rluc activity was determined. As shown in Fig. 3B, m4/7 replicated as efficiently as a WT replicon.

To further investigate the efficiency of m4/7 in supporting replication, these mutations were inserted into a replicon without a reporter gene (identical to the constructs shown in Fig. 3A, except for the lack of a reporter gene) to examine their effect in a multicycle replication system. To this end, the WT and CS mutant replicon RNAs without a Rluc reporter gene were electroporated into BHK packaging cells, BHK(VEErep/C*-E/Pac), expressing the WNV structural proteins C, prM, and E to produce VLPs (14). The resultant culture supernatants were harvested, and side-by-side focus formation assays of WT and m4/7 VLPs on BHK(VEErep/C*-E/Pac) cells were performed. As shown in Fig. 3C, these VLPs produced foci indistinguishable in size, indicating that the m4/7 RNAs were very similar to WT sequences in their ability to support the RNA replication needed for all steps of the viral life cycle. Coincidentally, these mutations demonstrated that the m4/7 mutation did not interfere with WNV genome packaging in this trans-packaging system for testing multicycle replication. Titers (focus-forming units) of VLPs recovered in supernatants from electroporated packaging cells were also indistinguishable between WT and m4/7 (data not shown), providing additional support for the similarity of WT and m4/7 in supporting RNA genome replication in this WNR.

Introduction of CS mutation into virus. In the VLP experiments described above, the CS mutant replicon m4/7 encoded a C protein with two amino acid substitutions at positions which are otherwise highly conserved among mosquito-borne flaviviruses. However, these VLP studies did not demonstrate whether these amino acid substitutions in C resulting from the m4/7 mutation affected viral replication, since authentic C protein was provided by the Venezuelan equine encephalitis virus replicon in BHK(VEErep/C*-E/Pac) cells. To examine the effect of CS mutation as well as alteration of the C protein on the replication of WNV, we introduced the m4/7 CS mutations into a full-length WNV genome (Fig. 4A). Recombinant WNV and infectious virus containing the m4/7 mutation were pre-

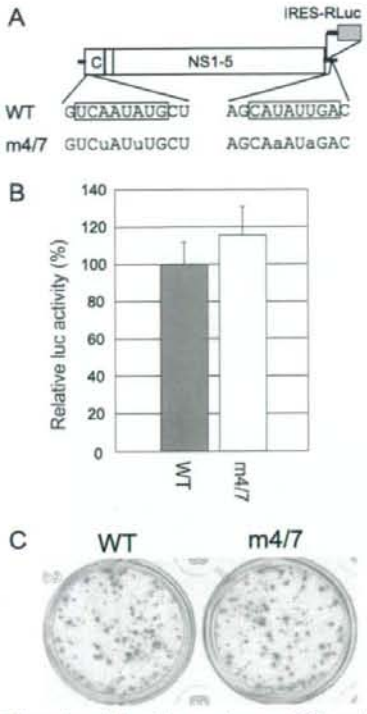

FIG. 3. Effect of multiple CS mutations on RNA replication and viral genome packaging. (A) Schematic representation of WNR RNA structure. The nucleotide sequences of CS are given next to their names. Boxes indicate the eight nucleotides that are 100% conserved among all mosquito-borne flaviviruses. Nucleotide substitutions in the 5′ CS and 3′ CS are in lower case. (B) RNA replication of WT and mutant replicon in BHK cells. Averages of triplicate relative luciferase activities at 2 days posttransfection were normalized to that at 5 h, and the WT control value was set to 100%; error bars show standard deviations. The experiment was repeated at least twice, producing similar results. (C) Photograph of monolayers of BHK packaging cells infected with WT or m4/7 mutant VLP, overlaid with semisolid medium, fixed, and immunostained with anti-NS1 antibody 48 h after incubation at 37°C.

pared, and side-by-side growth curves were generated with these viruses in BHK, Vero, and C7/10 cells (Fig. 4B).

Although mutated virus (m4/7) had two amino acid changes in the N-terminal C protein as well as both 5′-CS and 3′-CS mutations, we were unable to detect any dysfunction in its ability to replicate in either mammalian or mosquito cells (Fig. 4B). We also examined the focus phenotypes of these viruses on these cells, and both viruses formed similar-sized foci on monolayers of all three cell types (Fig. 4C), a finding that was particularly surprising in light of the absolute conservation of these sequences in all mosquito-borne flaviviruses sequenced to date.

These results, which show that m4/7 sequence was able to promote efficient replication of WNV, indicate that there is also no need to conserve this region of the C protein, since the m4/7 changes that altered the codons at these positions had no apparent effect on C protein function in viral genome replication and packaging.

Replicons containing two base substitutions only in 5′ CS or only in 3′ CS showed no RNA replication activity. Although the predicted RNA base pairings between the 5′ and 3′ CS of m4/7 were similar to those produced by WT CS (Fig. 5A), the predicted base pairing in genomes containing position 4 and position 7 mutations in the 5′ CS only or the 3′ CS only were dramatically different from those of WT and m4/7. To examine the effect of these unmatched double mutations on RNA replication, transcribed replicon RNAs containing these unmatched mutations were introduced into BHK cells, and Rluc activities were determined. As shown in Fig. 5B, replicons containing two base substitutions only in the 5′ CS (m4/7-5′) or only in the 3′ CS (m4/7-3′) showed no detectable RNA replication activity at the 48-h time point.

Specific infectivities of WT and mutated replicon RNA without the reporter gene were also determined by serially diluting BHK packaging cells electroporated with transcribed replicon RNAs in naïve packaging cells, and incubating these mixtures for 48 h at 37°C under semisolid medium. After 48 h, cells were fixed and stained with anti-NS1 antibody. As shown in Fig. 5A, the genomes with unmatched CS were over 10,000 times less efficient at producing focus formation in BHK packaging cells, whereas replicon RNA with WT and m4/7 sequences of both 5′ and 3′ CS produced the same number of infectious foci.

Although replicons with unmatched CS (m4/7-5′ and m4/7-3′) showed no detectable foci at 48 h posttransfection, repeated passaging of the supernatant from transfected BHK(VEErep/C*-E/Pac) cells with a longer incubation period (4 days) enabled us to rescue viable replicons from both WNR-CNS1-5 m4/7-5′ and m4/7-3′ RNA-transfected cells. To identify the nucleotide sequence in the CS region of these rescued replicons, supernatants from a second passage were used to infect BHK cells, and replicon RNAs were collected from the cells and reverse transcribed into cDNA. After PCR amplification, sequence analyses of the CS regions were performed. As shown in Fig. 5C, the rescued replicon population recovered from the m4/7-5′ transfection appeared to be homogeneous and contained a 1-base reversion at position 4 (U to A) of the 5′ CS, producing a CS with a single unmatched position equivalent to an m7 mutation in the 5′ CS that was unable to pair with the WT 3′ CS in the genomes found in this rescued population. The replicon population rescued from the m4/7-3′ transfection contained reversions at position 4 (A to U) and position 7 (A to U). Both nucleotide positions appeared to contain mixtures of both original (transfected mutant RNA) and revertants to the WT nucleotide. It is likely that these represented mixtures of genomes with reversions at one position or the other; thus, the rescued population was likely to contain two different genomes, one with an m4 mutation in its 3′ CS and the other with an m7 mutation in its 3′ CS. It is interesting that replicons rescued from m4/7-5′ or m4/7-3′ showed nucleotide changes in mutated positions but not the WT portion of the CS. It should be noted that sequencing of similar blind-passaged WT and m4/7 WNRs did not reveal any nucleotide changes in their CS (Fig. 5C).

Production of single-cycle WNV with two-component genomes. Identification of mutated CS that permitted the efficient replication of WNV genome encouraged us to examine

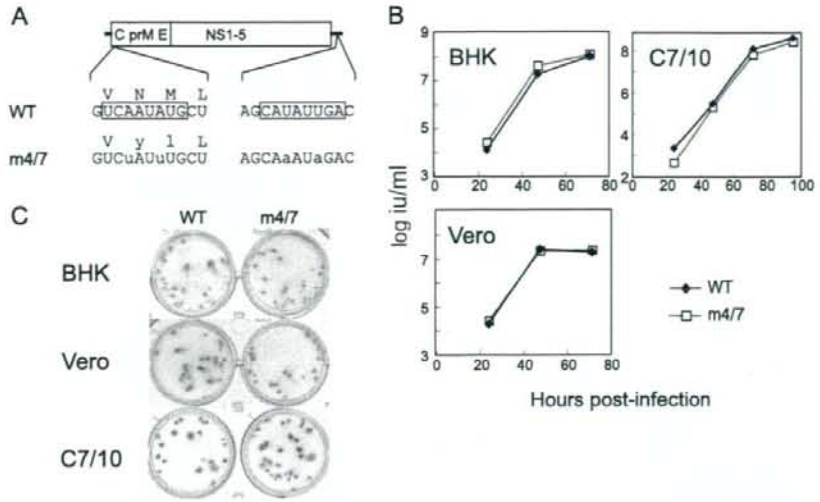

FIG. 4. Effect of multiple CS mutations on growth kinetics of recombinant virus. (A) Schematic representation of WNV RNA structure. The nucleotide sequences of CS and coding amino acid sequences are indicated next to their names. Nucleotide substitutions at 5′ CS and 3′ CS and substituted amino acid in the C-coding region are indicated in lower case. Boxes indicate the eight nucleotides that are 100% conserved among all mosquito-borne flaviviruses. (B) Growth curves of WT and mutant virus on BHK, Vero, and C7/10 cells. Monolayers of cells were infected with the indicated virus at an MOI of 0.05 for BHK and Vero cells and an MOI of 0.2 for C7/10 cells. At each time point, the media were removed and frozen for subsequent titration and fresh media were added. Virus titers in cell culture media were determined on Vero cells. (C) Photograph of monolayers BHK, Vero, and C7/10 cells infected with WT or m4/7 recombinant virus, overlaid with semisolid media, fixed at 40 h postinfection for BHK and Vero cells and 72 h postinfection for C7/10 cells, and immunostained with anti-WNV antibody.

their use in producing a two-component LAV based on our single-cycle WNV, named RepliVAX WN. The RepliVAX WN genome has a large deletion in the C-coding sequence so that it can be packaged only in C-expressing cell lines (28, 44). Recently we reported that a C-expressing flavivirus replicon can also complement RepliVAX genomes (39). However, there is a concern that intergenomic recombination between the two flavivirus genomes could produce a live infectious agent during LAV production or in LAV-vaccinated individuals. Although such an event is unlikely, this recombination potential could be significantly reduced by utilizing genomes with different pairs of CS, ensuring that recombinant genomes would not be replicationally active. To test if the m4/7 CS could be used for this purpose, we designed the C protein-expressing WNV helper genome (Fig. 6A) to contain these mutant CS. Based on work with the two-component YFV system indicating that helper genomes encoding the WT C gene did not efficiently complement RepliVAX genomes (39), we constructed our WNV helper genomes with a truncated C gene followed by the gene for the FMDV autoproteinase 2A, a codon-optimized synthetic C gene, and the nonstructural protein genes (Fig. 6A). As expected, this genome was packaged into particles by cells expressing WNV prM/E from a Venezuelan equine encephalitis virus replicon, and helper genome packaging was dependent on cell line-expressed prM/E but did not require cell-expressed C (results not shown), demonstrating that the cassette comprising the FMDV autoproteinase and the codon-optimized C gene was able to supply a functional C protein. When VLPs (referred to here as helper particles) containing this helper genome that were recovered from packaging cells were mixed with RepliVAX WN.2 particles at an equal multiplicity, they were able to grow to high titers in Vero cells (Fig. 6B). The titer of these particles after repeated passage also remained high (Fig. 6C). These data indicate that the m4/7 CS mutations could be utilized for generating a two-component WNV LAV vaccine candidate with a reduced recombination potential.

DISCUSSION

In this study, we set out to identify unnatural CS that were capable of supporting efficient replication of the flavivirus genome so that these sequences could be utilized to enhance the safety of flavivirus LAV. Previous studies indicated that the complementarity of CS, rather than precise nucleotide sequences, was a prerequisite for flavivirus RNA replication (2, 13, 19, 27), but these studies also showed that viral genomes with complementary but unnatural CS replicated more poorly than WT genomes. Due to the nature of the mutant sequences reported in those works, it is unclear if the levels of replication achieved by genomes harboring these matched mutations were the result of the predicted free energy of the interactions between the mutated 5′ CS and 3′ CS of the genome or the precise nucleotide sequences selected for insertion in the reported mutant CS. To circumvent this problem, we undertook large-scale mutagenesis studies of the CS of WNV that preserved the predicted free energies of interaction between the 5′ and 3′ CS in order to find mutant CS that would support WT levels of genome replication.

To produce CS with an inability to revert to WT sequences

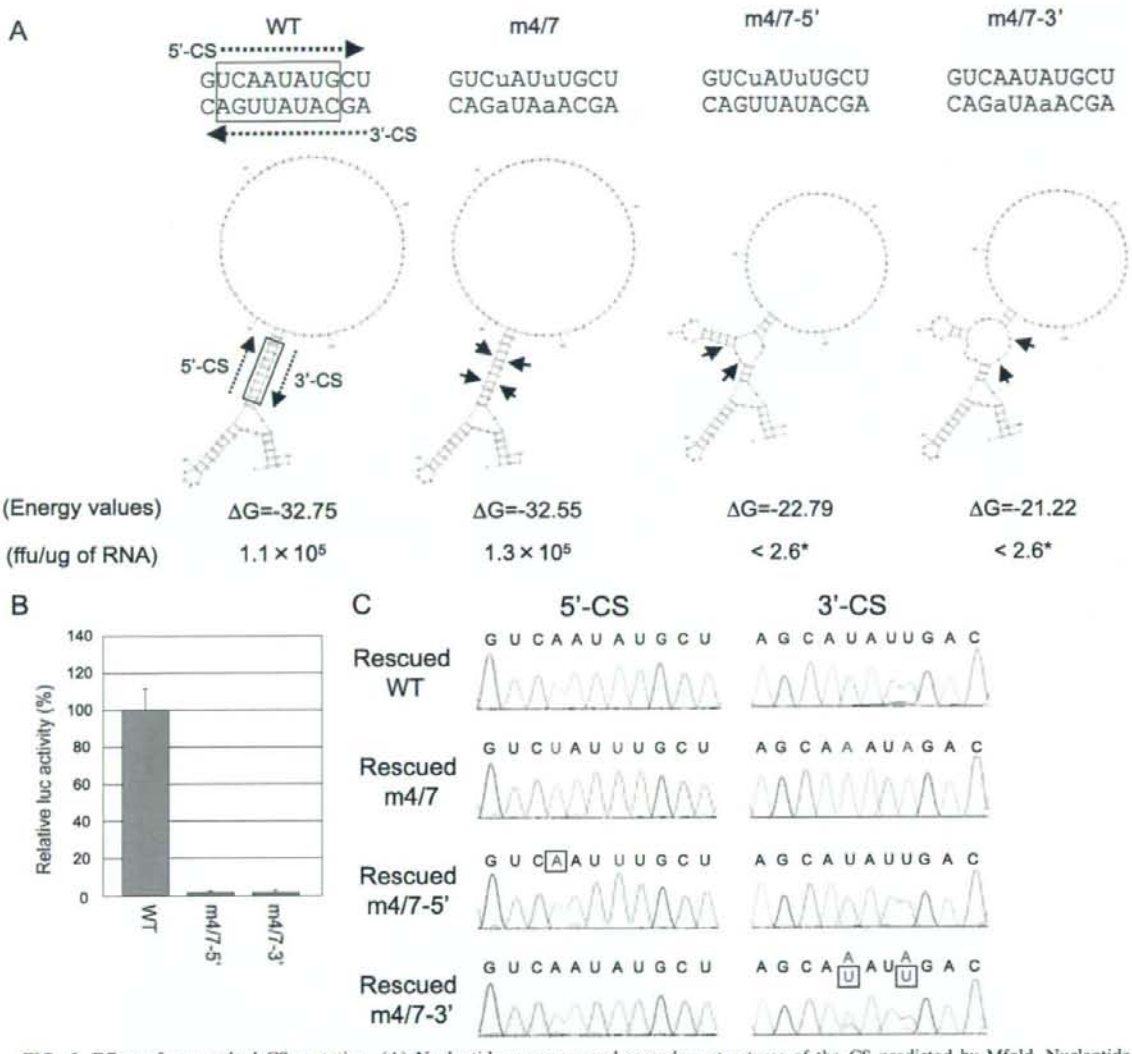

FIG. 5. Effect of unmatched CS mutation. (A) Nucleotide sequence and secondary structures of the CS predicted by Mfold. Nucleotide substitutions at 5′ CS and 3′ CS are in lower case. Dotted arrows show the 5′-to-3′ direction of nucleotide in CS. Short arrows indicate nucleotide positions with substitutions. The ΔG values and the structures were produced using an artificial sequence created by fusing 52 bases of C coding region, 31 bases of 3′ UTR, and a 38-nucleotide A stuffer. The numbers of focus-forming units (ffu) per microgram of electroporated RNA are also indicated. Asterisks show no detection of foci. The limit of detection for this assay was 2.6 focus-forming units/μg. (B) RNA replication of unmatched CS mutant replicons in BHK cells. Average triplicate relative luciferase activities at 2 days posttransfection were normalized to those at 5 h, and the WT control value was set to 100%; error bars show standard deviations. The experiment was repeated at least twice, with consistent results. (C) Electropherograms showing the sequences of the blind-passed replicons derived from WT, m4/7, m4/7-5′, and m4/7-3′. The nucleotide sequences of the CS are indicated above the electropherograms. Deliberately mutated CS nucleotides are shown in red; changes from these mutations detected in rescued populations are shown in red and boxed in black.

in the rare event of recombination with WT CS, we introduced a series of nonconservative multiple base changes within the CS, in such a manner that the mutations thus produced did not alter the overall structure or predicted free energy of the interaction between the 5′ and 3′ CS. Surprisingly, none of these mutant sequences supported detectable WNR genome replication levels, indicating that there were position-specific requirements suggested by earlier studies (see the introduction). To systematically identify sites that could be mutated, we then undertook a site-by-site mutation strategy in which we independently switched each A-U pair to a U-A, each U-A to an A-U, each G-C to a C-G, and each C-G to a G-C of the 5′ and 3′ CS. As expected, this strategy indicated that swaps at certain positions (discussed in detail below) were highly deleterious,

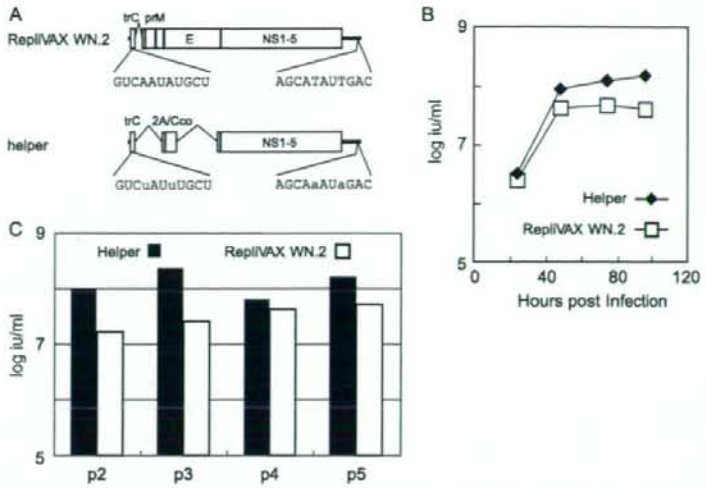

FIG. 6. Analysis of two-component genome replication. (A) Schematic representation of RepliVAX WN.2 and helper genome structure showing the position and composition of the WT (RepliVAX WN.2) and mutant (helper) CS. Nucleotide substitutions at 5′ CS and 3′ CS are in lower case. (B) Release of infectious particles containing the genome of RepliVAX WN.2 or helper from Vero cells infected with a mixture of particles at an MOI of 0.5. The titers of particles recovered at each time point were determined by an infectious-unit assay performed on Vero cells (see Materials and Methods). The titer of the RepliVAX WN.2 particles was determined by focus formation assays using an E protein-specific serum that detects only cells infected with the E-encoding RepliVAX WN.2 genome. The titer of helper particles was determined by subtraction of the focus formation assay titer of RepliVAX WN.2 from the combined titer of RepliVAX WN.2 and helper particles determined by using an anti-WNV serum (see Materials and Methods). (C) Titers of infectious particles containing the genome of RepliVAX WN.2 and helper after serial passage in Vero cells. Supernatants collected 3 days postinfection were used to inoculate fresh Vero cells. This procedure was repeated five times, and the titers of both helper and RepliVAX WN.2 in each passage were determined as described for panel B.

whereas some paired mutations produced WT levels of RNA replication.

Although the introduction of these singly mutated CS pairs into a flavivirus LAV would be expected to reduce its ability to produce a viable recombinant with WT virus, we sought to further reduce the possibility of generation of viable recombinants by combining mutations. Interestingly, the combination of two mutations into paired CS resulted in the production of WNR genomes that appeared to replicate at WT levels when introduced into BHK cells. To analyze these genomes in a multistep growth situation, we further compared their ability to replicate in a packaging cell system that should have reduced the effect of C-protein coding changes (that resulted from the CS mutations) on WNR packaging and spread. Using this system, we were unable to detect any differences between the replication (and packaging) activity of WT and the paired double-mutated-CS-bearing WNR.

Due to the highly conserved nature of the CS in all mosquito-borne flaviviruses, we were surprised by our ability to easily generate mutated CS with apparent WT levels of replication activity. To further test their ability to support WT levels of replication, the paired double CS mutations were introduced into an infectious WNV. When this virus was compared to its parental cDNA-derived WNV, it displayed indistinguishable growth properties in low-multiplicity single-cycle growth assays in two different mammalian cell liens, as well as in a mosquito cell culture. Since the CS changes we had selected based on replicational activity produced changes in the encoded C protein, our studies showing that viruses with mutated C proteins are highly efficient in their replication also demonstrate that the high level of amino acid conservation in C in the region that overlaps the 5′ CS is due not to a constraint on C protein structure but rather to a constraint on complementarity of the 5′ and 3′ CS. These data are consistent with reports from trans-packaging studies demonstrating that deletion of the C coding sequence corresponding to 5′ CS did not prevent packaging of replicon genome of YFV (33) or WNV (37). Nevertheless, as discussed below, some of the activities of the C protein might be affected by mutations of the CS, complicating analyses of this busy portion of the flavivirus genome.

A direct analysis of WNR containing a combination of WT and either 5′ or 3′ double-mutant CS demonstrated that the intentional combination of these unmatched CS produced genomes that displayed undetectable levels of genome replication. However, blind passage of cells transfected with large amounts of these genomes resulted in rescue of replicationally active genomes that had undergone mutation. The nucleotide sequence analyses of these genomes showed that replicationally active genomes contained reversions in at least one of the mismatched positions. These data indicate that replicons with a single noncomplementary base pair at either the m4 or m7 position were viable, consistent with our findings that genomes with a single, noncomplementary mutation in position 2 (m2-5′) were replicationally active. In contrast, WNR with our CS mutant m4/7 was stably maintained for multiple passages, indicating that the m4/7 mutation is not under strong selective pressure, consistent with its WT levels of replication. These

data suggest that the m4/7 mutation is suitable for use in the design of LAV.

As part of our studies to systematically identify mutations in the 5′ and 3′ CS that could support efficient replication, we were surprised to find two mutants (m1 and m2) for which a single pair of swaps of the nucleotides in the first or second positions, respectively, of the paired CS abolished replication. Studies with replicons containing mutations at these positions in only the 5′ or only the 3′ CS revealed that the precise nucleotides at the 3′-CS positions were more critical for replication than the corresponding 5′-CS nucleotides. These data suggesting that these 3′ CS play a critical role in RNA replication, either by themselves or as part of other local secondary structures.

Recently, it was reported that JEV C protein was processed by cathepsin L, which is associated with replication of JEV in neural and macrophage cells (30). Whether WNV C is also processed by cathepsin L and/or whether this processing is important for replication of WNV has not been determined, but the C protein sequences of these two viruses are nearly identical at the predicted cathepsin L cleavage site. The possibility that the C mutants created in our study had an effect on the processing of C by cathepsin L cannot be ruled out based on our studies. In the case of m1 and m2, both mutations generated amino acid changes at five codons upstream of the predicted cathepsin L cleavage site (V to L in m1 and V to D in m2). However, m2-5′, which also contains the same amino acid substitutions as m2, showed only a slight reduction of RNA replication compared to that of WT genomes, indicating that these mutations in coding capacity, which could alter cathepsin L cleavage, do not have a serious effect on genome replication in our system. These results further support the possibility that the nucleotide sequence in CS is critical for efficient RNA replication, whereas the encoded protein sequences are not as critical (see above).

One stimulus for initiation of these studies was the concern that LAV for flaviviruses, especially those that carried foreign genes, could recombine with viruses in nature (38). To date, there is no evidence that this type of recombination has occurred; however, in the case of the distantly related poliovirus, recombinants between LAV and wild viruses have been identified in nature (4, 15). Recombination between a vaccine strain and persisting pestivirus, generating cytopathogenic virus and inducing lethal disease in cattle, has also been reported (5). We believe that the utilization of WNV LAV with the CS mutant that we have identified would provide an additional level of safety for LAV use, since these CS mutations would reduce the viability of recombinants with WT viruses. For similar reasons, our CS mutations also have a significant advantage in the production of a new class of vaccines recently described by Shustov et al. (39). These vaccines consist of a single-cycle virus (named RepliVAX) which encodes a C-gene-deleted genome that can be cocultivated with a helper genome encoding the C but not prM/E proteins (39). Although Shustov et al. did not detect any infectious full-length virus in cells forced to replicate both RepliVAX and its helper genome (39), the in vitro cocultivation of this type of vaccine could be rendered safer by utilizing CS mutations of the type we have identified here. Preliminary studies presented in this work demonstrate that repeated cocultivation of RepliVAX WN with a helper encoding mutant CS can be accomplished, documenting the utility of CS mutants in a practical application.

In conclusion, we demonstrated the systematic evaluation of mutated CS on replication of WNV and identified mutant CS that permitted efficient replication of the WNV genome in both WNR and infectious virus. The WNR containing a combination of WT and either 5′ or 3′ mutant CS was very inefficient at producing a replicationally active genome. Therefore, recombinant genomes that arose from a single recombination event between LAV carrying these types of mutant CS and natural viruses would not be replicationally active. Thus, these studies demonstrated that the high level of replication of mutated CS genome could be used to enhance the safety of existing flavivirus LAV as well as enhance the safety of production and use of a recently described LAV based on two genomes with complementary packaging (39).

ACKNOWLEDGMENTS

We thank E. Konishi (Kobe University) for providing the anti-NS1 antibody. We also thank D. Widman (UTMB) for supplying the RepliVAX WN.2.

This work was supported by a grant from NIAID to P.W.M. through the Western Regional Center of Excellence for Biodefense and Emerging Infectious Disease Research (NIH grant U54 AI057156).

REFERENCES

1. **Ackermann, M., and R. Padmanabhan.** 2001. De novo synthesis of RNA by the dengue virus RNA-dependent RNA polymerase exhibits temperature dependence at the initiation but not elongation phase. J. Biol. Chem. **276:** 39926–39937.
2. **Alvarez, D. E., A. L. De Lella Ezcurra, S. Fucito, and A. V. Gamarnik.** 2005. Role of RNA structures present at the 3′UTR of dengue virus on translation, RNA synthesis, and viral replication. Virology **339:**200–212.
3. **Alvarez, D. E., M. F. Lodeiro, S. J. Luduena, L. I. Pietrasanta, and A. V. Gamarnik.** 2005. Long-range RNA-RNA interactions circularize the dengue virus genome. J. Virol. **79:**6631–6643.
4. **Arita, M., S. L. Zhu, H. Yoshida, T. Yoneyama, T. Miyamura, and H. Shimizu.** 2005. A Sabin 3-derived poliovirus recombinant contained a sequence homologous with indigenous human enterovirus species C in the viral polymerase coding region. J. Virol. **79:**12650–12657.
5. **Becher, P., M. Orlich, and H. J. Thiel.** 2001. RNA recombination between persisting pestivirus and a vaccine strain: generation of cytopathogenic virus and induction of lethal disease. J. Virol. **75:**6256–6264.
6. **Best, S. M., K. L. Morris, J. G. Shannon, S. J. Robertson, D. N. Mitzel, G. S. Park, E. Boer, J. B. Wolfinbarger, and M. E. Bloom.** 2005. Inhibition of interferon-stimulated JAK-STAT signaling by a tick-borne flavivirus and identification of NS5 as an interferon antagonist. J. Virol. **79:**12828–12839.
7. **Blaney, J. E., Jr., A. P. Durbin, B. R. Murphy, and S. S. Whitehead.** 2006. Development of a live attenuated dengue virus vaccine using reverse genetics. Viral Immunol. **19:**10–32.
8. **Blaney, J. E., Jr., N. S. Sathe, L. Goddard, C. T. Hanson, T. A. Romero, K. A. Hanley, B. R. Murphy, and S. S. Whitehead.** 2008. Dengue virus type 3 vaccine candidates generated by introduction of deletions in the 3′ untranslated region (3′-UTR) or by exchange of the DENV-3 3′-UTR with that of DENV-4. Vaccine **26:**817–828.
9. **Bourne, N., F. Scholle, M. C. Silva, S. L. Rossi, N. Dewsbury, B. Judy, J. B. De Aguiar, M. A. Leon, D. M. Estes, R. Fayzulin, and P. W. Mason.** 2007. Early production of type I interferon during West Nile virus infection: role for lymphoid tissues in IRF3-independent interferon production. J. Virol. **81:**9100–9108.
10. **Bredenbeek, P. J., E. A. Kooi, B. Lindenbach, N. Huijkman, C. M. Rice, and W. J. Spaan.** 2003. A stable full-length yellow fever virus cDNA clone and the role of conserved RNA elements in flavivirus replication. J. Gen. Virol. **84:**1261–1268.
11. **Brinton, M. A., A. V. Fernandez, and J. H. Dispoto.** 1986. The 3′-nucleotides of flavivirus genomic RNA form a conserved secondary structure. Virology **153:**113–121.
12. **Burke, D. S., and T. P. Monath.** 2001. Flaviviruses, p. 1043–1125. *In* D. M. Knipe, P. M. Howley, D. G. Griffin, R. A. Lamb, M. A. Martin, and B. Roizman (ed.), Fields virology, 4th ed., vol. 1. Lippincott Williams & Wilkins, Philadelphia, Pa.
13. **Corver, J., E. Lenches, K. Smith, R. A. Robison, T. Sando, E. G. Strauss, and J. H. Strauss.** 2003. Fine mapping of a *cis*-acting sequence element in yellow

fever virus RNA that is required for RNA replication and cyclization. J. Virol. **77:**2265–2270.
14. **Fayzulin, R., F. Scholle, O. Petrakova, I. Frolov, and P. W. Mason.** 2006. Evaluation of replicative capacity and genetic stability of West Nile virus replicons using highly efficient packaging cell lines. Virology **351:**196–209.
15. **Guillot, S., V. Caro, N. Cuervo, E. Korotkova, M. Combiescu, A. Persu, A. Aubert-Combiescu, F. Delpeyroux, and R. Crainic.** 2000. Natural genetic exchanges between vaccine and wild poliovirus strains in humans. J. Virol. **74:**8434–8443.
16. **Guirakhoo, F., S. Kitchener, D. Morrison, R. Forrat, K. McCarthy, R. Nichols, S. Yoksan, X. Duan, T. H. Ermak, N. Kanesa-Thasan, P. Bedford, J. Lang, M. J. Quentin-Millet, and T. P. Monath.** 2006. Live attenuated chimeric yellow fever dengue type 2 (ChimeriVax-DEN2) vaccine: phase I clinical trial for safety and immunogenicity: effect of yellow fever pre-immunity in induction of cross neutralizing antibody responses to all 4 dengue serotypes. Hum. Vaccine **2:**60–67.
17. **Hahn, C. S., Y. S. Hahn, C. M. Rice, E. Lee, L. Dalgarno, E. G. Strauss, and J. H. Strauss.** 1987. Conserved elements in the 3′ untranslated region of flavivirus RNAs and potential cyclization sequences. J. Mol. Biol. **198:**33–41.
18. **Huang, C. Y., S. J. Silengo, M. C. Whiteman, and R. M. Kinney.** 2005. Chimeric dengue 2 PDK-53/West Nile NY99 viruses retain the phenotypic attenuation markers of the candidate PDK-53 vaccine virus and protect mice against lethal challenge with West Nile virus. J. Virol. **79:**7300–7310.
19. **Khromykh, A. A., H. Meka, K. J. Guyatt, and E. G. Westaway.** 2001. Essential role of cyclization sequences in flavivirus RNA replication. J. Virol. **75:**6719–6728.
20. **Kitai, Y., M. Shoda, T. Kondo, and E. Konishi.** 2007. Epitope-blocking enzyme-linked immunosorbent assay to differentiate West Nile virus from Japanese encephalitis virus infections in equine sera. Clin. Vaccine Immunol. **14:**1024–1031.
21. **Kitchener, S., M. Nissen, P. Nasveld, R. Forrat, S. Yoksan, J. Lang, and J. F. Saluzzo.** 2006. Immunogenicity and safety of two live-attenuated tetravalent dengue vaccine formulations in healthy Australian adults. Vaccine **24:**1238–1241.
22. **Kummerer, B. M., and C. M. Rice.** 2002. Mutations in the yellow fever virus nonstructural protein NS2A selectively block production of infectious particles. J. Virol. **76:**4773–4784.
23. **Lin, R. J., B. L. Chang, H. P. Yu, C. L. Liao, and Y. L. Lin.** 2006. Blocking of interferon-induced Jak-Stat signaling by Japanese encephalitis virus NS5 through a protein tyrosine phosphatase-mediated mechanism. J. Virol. **80:**5908–5918.
24. **Lindenbach, B. D., and C. M. Rice.** 2001. *Flaviviridae*: the viruses and their replication, p. 991–1041. *In* D. M. Knipe, P. M. Howley, D. G. Griffin, R. A. Lamb, M. A. Martin, and B. Roizman (ed.), Fields virology, 4th ed., vol. 1. Lippincott Williams & Wilkins, Philadelphia, Pa.
25. **Liu, W. J., H. B. Chen, and A. A. Khromykh.** 2003. Molecular and functional analyses of Kunjin virus infectious cDNA clones demonstrate the essential roles for NS2A in virus assembly and for a nonconservative residue in NS3 in RNA replication. J. Virol. **77:**7804–7813.
26. **Liu, W. J., X. J. Wang, V. V. Mokhonov, P. Y. Shi, R. Randall, and A. A. Khromykh.** 2005. Inhibition of interferon signaling by the New York 99 strain and Kunjin subtype of West Nile virus involves blockage of STAT1 and STAT2 activation by nonstructural proteins. J. Virol. **79:**1934–1942.
27. **Lo, M. K., M. Tilgner, K. A. Bernard, and P. Y. Shi.** 2003. Functional analysis of mosquito-borne flavivirus conserved sequence elements within 3′ untranslated region of West Nile virus by use of a reporting replicon that differentiates between viral translation and RNA replication. J. Virol. **77:**10004–10014.
28. **Mason, P. W., A. V. Shustov, and I. Frolov.** 2006. Production and characterization of vaccines based on flaviviruses defective in replication. Virology **351:**432–443.
29. **Monath, T. P., J. Liu, N. Kanesa-Thasan, G. A. Myers, R. Nichols, A. Deary, K. McCarthy, C. Johnson, T. Ermak, S. Shin, J. Arroyo, F. Guirakhoo, J. S. Kennedy, F. A. Ennis, S. Green, and P. Bedford.** 2006. A live, attenuated recombinant West Nile virus vaccine. Proc. Natl. Acad. Sci. USA **103:**6694–6699.
30. **Mori, Y., T. Yamashita, Y. Tanaka, Y. Tsuda, T. Abe, K. Moriishi, and Y. Matsuura.** 2007. Processing of capsid protein by cathepsin L plays a crucial role in replication of Japanese encephalitis virus in neural and macrophage cells. J. Virol. **81:**8477–8487.
31. **Munoz-Jordan, J. L., M. Laurent-Rolle, J. Ashour, L. Martinez-Sobrido, M. Ashok, W. I. Lipkin, and A. Garcia-Sastre.** 2005. Inhibition of alpha/beta interferon signaling by the NS4B protein of flaviviruses. J. Virol. **79:**8004–8013.
32. **Munoz-Jordan, J. L., G. G. Sanchez-Burgos, M. Laurent-Rolle, and A. Garcia-Sastre.** 2003. Inhibition of interferon signaling by dengue virus. Proc. Natl. Acad. Sci. USA **100:**14333–14338.
33. **Patkar, C. G., C. T. Jones, Y. H. Chang, R. Warrier, and R. J. Kuhn.** 2007. Functional requirements of the yellow fever virus capsid protein. J. Virol. **81:**6471–6481.
34. **Pletnev, A. G., M. S. Claire, R. Elkins, J. Speicher, B. R. Murphy, and R. M. Chanock.** 2003. Molecularly engineered live-attenuated chimeric West Nile/dengue virus vaccines protect rhesus monkeys from West Nile virus. Virology **314:**190–195.
35. **Pletnev, A. G., D. E. Swayne, J. Speicher, A. A. Rumyantsev, and B. R. Murphy.** 2006. Chimeric West Nile/dengue virus vaccine candidate: preclinical evaluation in mice, geese and monkeys for safety and immunogenicity. Vaccine **24:**6392–6404.
36. **Rossi, S. L., Q. Zhao, V. K. O'Donnell, and P. W. Mason.** 2005. Adaptation of West Nile virus replicons to cells in culture and use of replicon-bearing cells to probe antiviral action. Virology **331:**457–470.
37. **Scholle, F., Y. A. Girard, Q. Zhao, S. Higgs, and P. W. Mason.** 2004. trans-Packaged West Nile virus-like particles: infectious properties in vitro and in infected mosquito vectors. J. Virol. **78:**11605–11614.
38. **Seligman, S. J., and E. A. Gould.** 2004. Live flavivirus vaccines: reasons for caution. Lancet **363:**2073–2075.
39. **Shustov, A. V., P. W. Mason, and I. Frolov.** 2007. Production of pseudoinfectious yellow fever virus with a two-component genome. J. Virol. **81:**11737–11748.
40. **Sun, W., A. Nisalak, M. Gettayacamin, K. H. Eckels, J. R. Putnak, D. W. Vaughn, B. L. Innis, S. J. Thomas, and T. P. Endy.** 2006. Protection of Rhesus monkeys against dengue virus challenge after tetravalent live attenuated dengue virus vaccination. J. Infect. Dis. **193:**1658–16565.
41. **Suzuki, R., L. de Borba, C. N. Duarte dos Santos, and P. W. Mason.** 2007. Construction of an infectious cDNA clone for a Brazilian prototype strain of dengue virus type 1: characterization of a temperature-sensitive mutation in NS1. Virology **362:**374–383.
42. **Weaver, S. C., and A. D. Barrett.** 2004. Transmission cycles, host range, evolution and emergence of arboviral disease. Nat. Rev. Microbiol. **2:**789–801.
43. **Wengler, G., and E. Castle.** 1986. Analysis of structural properties which possibly are characteristic for the 3′-terminal sequence of the genome RNA of flaviviruses. J. Gen. Virol. **67:**1183–1188.
44. **Widman, D. G., T. Ishikawa, R. Fayzulin, N. Bourne, and P. W. Mason.** 2008. Construction and characterization of a second-generation pseudoinfectious West Nile virus vaccine propagated using a new cultivation system. Vaccine **26:**2762–2771.
45. **Zhang, B., H. Dong, D. A. Stein, P. L. Iversen, and P. Y. Shi.** 2008. West Nile virus genome cyclization and RNA replication require two pairs of long-distance RNA interactions. Virology **373:**1–13.
46. **Zuker, M.** 2003. Mfold web server for nucleic acid folding and hybridization prediction. Nucleic Acids Res. **31:**3406–3415.

Available online at www.sciencedirect.com
ScienceDirect
Journal of Virological Methods 148 (2008) 174–181
Journal of Virological Methods
www.elsevier.com/locate/jviromet

Dynamic behavior of hepatitis C virus quasispecies in a long-term culture of the three-dimensional radial-flow bioreactor system

Kyoko Murakami [a], Yasushi Inoue [a,b], Su-Su Hmwe [a,c], Kazuhiko Omata [a,d], Tomokatsu Hongo [e], Koji Ishii [a], Sayaka Yoshizaki [a], Hideki Aizaki [a], Tomokazu Matsuura [f], Ikuo Shoji [a], Tatsuo Miyamura [a], Tetsuro Suzuki [a,*]

[a] *Department of Virology II, National Institute of Infectious Diseases, 1-23-1 Toyama, Shinjuku-ku, Tokyo 162-8640, Japan*
[b] *Pulmonary and Critical Care Unit, Mita Hospital, International University of Health and Welfare, Japan*
[c] *Department of Infectious Diseases, Internal Medicine, Graduate School of Medicine, University of Tokyo, Tokyo, Japan*
[d] *Department of Oral and Maxillofacial Surgery, The Nippon Dental University School of Dentistry at Tokyo, Tokyo, Japan*
[e] *ABLE Corporation, Shizuoka, Japan*
[f] *Department of Laboratory medicine, The Jikei University School of Medicine, Tokyo, Japan*

Received 25 July 2007; received in revised form 9 November 2007; accepted 21 November 2007

Abstract

Hepatitis C virus (HCV) exists in infected individuals as quasispecies, usually consisting of a dominant viral isolate and a variable mixture of related, yet genetically distinct, variants. A prior HCV infection system was developed using human hepatocellular carcinoma cells cultured in the three-dimensional radial-flow bioreactor (RFB), in which the cells retain morphological appearance and their differentiated hepatocyte functions for an extended period of time. This report studies the selection and alteration of the viral quasispecies in the RFB system inoculated with pooled serum derived from HCV carriers. Monitoring the viral RNA and core protein in the culture supernatants, together with nucleotide sequencing of hypervariable region 1 of the HCV genome, demonstrated that (1) the virus production intermittently fluctuated in the cultures, (2) the viral genetic diversity was markedly reduced 3 days post-infection (p.i.), and (3) dominant species changed on days 19–33 p.i., suggesting that the virus populations can be selected according to susceptibility to the viral infection and replication. A therapeutic effect of interferon-α also demonstrated the inhibition of HCV expression. Thus, this HCV infection model in the RFB system should be useful for investigating the dynamic behavior of HCV quasispecies in cultured cells and evaluating anti-HCV compounds.

Keywords: Hepatitis C virus; Three-dimensional culture; Radial-flow bioreactor; Dynamics; Quasispecies

1. Introduction

Hepatitis C virus (HCV) is a major cause of chronic liver diseases (Choo et al., 1989; Kuo et al., 1989; Saito et al., 1990) and has been estimated to infect more than 170 million people throughout the world (Poynard et al., 2003). Symptoms of persistent HCV infection extend from chronic hepatitis to cirrhosis and ultimately hepatocellular carcinoma (Choo et al., 1989; Kuo et al., 1989; Saito et al., 1990). HCV belongs to the genus *Hepacivirus*, included in the family of Flaviviridae, and possesses a viral genome of a single, positive-stranded RNA with a nucleotide (nt) length of approximately 9.6 kb (Choo et al., 1991; Grakoui et al., 1993; Hijikata et al., 1991). It has been shown that HCV, like many other RNA viruses, circulates within infected individuals as a diverse population and closely related variants are referred to as quasispecies (Martell et al., 1992). This quasispecies model of mixed virus populations may imply a significant survival advantage because the simultaneous presence of multiple variant genomes and/or high rate of generation of new variants allow rapid selection of the mutants are better suited to new environmental conditions (Pawlotsky, 2006).

Studies on HCV replication and development of selective antiviral drugs have been hampered primarily by the lack of efficient cell culture systems. Establishment of selectable dicistronic HCV RNAs that are capable of autonomous replication to high levels in human hepatoma Huh-7 cells was a

* Corresponding author. Tel.: +81 3 5285 1111; fax: +81 3 5285 1161.
E-mail address: tesuzuki@nih.go.jp (T. Suzuki).

0166-0934/$ – see front matter © 2007 Elsevier B.V. All rights reserved.
doi:10.1016/j.jviromet.2007.11.001

significant breakthrough in HCV research; however, virus production has not been observed in the conventional monolayer cultures (Blight et al., 2000; Lohmann et al., 1999). Recently, it has been described that infectious HCV particles are efficiently produced from a genotype 2a isolate JFH-1 in Huh-7 cells (Blight et al., 2000; Wakita et al., 2005; Zhong et al., 2005). This JFH-1 based HCV culture system is an invaluable achievement permitting a variety of studies on the complete HCV life cycle. However, HCV infection systems with human sera or plasmas containing intact virions are still limited because of low levels of propagation in the cultures. Reverse transcription (RT)-PCR was typically used to detect the viral RNA in cell extracts; however, synthesized viral proteins were not observed in these systems (Ikeda et al., 1998; Tagawa et al., 1995).

There are reports of differentiated human hepatoma FLC4 (functional liver cell 4) cells grown in a three-dimensional (3D) radial-flow bioreactor (RFB) that can be infected by HCV-positive serum and support viral replication (Aizaki et al., 2003). Furthermore, production and release of infectious HCV has been observed in the RFB system following transfection of FLC4 cells with *in vitro* transcribed HCV genomic RNA, as well as in a 3D system using Huh-7 cells harboring genome-length dicistronic RNAs (Murakami et al., 2006). The RFB system, in which the bioreactor column consists of a cylindrical matrix with porous bead microcarriers extended vertically, was aimed initially at developing artificial liver tissues and allows liver-derived cells to maintain morphological appearance as well as their physiological functions, such as the ability to synthesize albumin and drug-metabolizing activity mediated by cytochrome P450 (Iwahori et al., 2003). The radial-flow configuration permits full contact between culture medium and cells at a physiologic perfusion flow rate, and prevents excessive shear stresses and buildup of waste products, thus ensuring the long-term viability of 3D cell culture.

The aim of the present study was to characterize HCV dynamics in the RFB system during long-term cultures inoculated with pooled serum obtained from HCV carriers, and to examine the therapeutic effects of interferon-alpha (IFN-α) in this HCV infection model.

2. Materials and methods

2.1. Cell cultures

FLC4 cells (Aoki et al., 1998), which were derived from human hepatocellular carcinoma cells and negative for HCV RNA and HBV DNA, were maintained in serum-free ASF104 medium (Ajinomoto, Japan) supplemented with 4 g/L D-glucose on the collagen-coated dishes before inoculating into the RFB column. The RFB system (ABLE, Japan) was manipulated as described previously (Aizaki et al., 2003) with minor modifications. Briefly, RFB columns, which have bed volumes of 30 or 4 mL and are filled with porous glass microcarriers (diameter 0.6 mm, vacant capacity 50%, pore size <120 μm) (Hongo et al., 2005), were seeded with FLC4 cells, which subsequently attached to the surface and inside of porous glass beads. ASF104 medium containing 2% fetal calf serum was added at a flow rate of 50 mL/day, and the culture condition was automatically controlled by monitoring temperature, pH value and oxygen levels in the vessel throughout the duration of the study.

2.2. Infection of HCV-positive sera

HCV antibody-positive sera used in this study were blood donor samples supplied by The Japanese Red Cross Center, Tokyo, Japan. HCV RNA loads in the sera were as follows: serum A, 2.4×10^6 copies/mL; serum B, 8.6×10^6 copies/mL; serum C, 5.9×10^6 copies/mL; serum D, 2.5×10^6 copies/mL; serum E, 1.0×10^7 copies/mL; serum F, 1.4×10^7 copies/mL (Table 1). In the first experiment (Fig. 3), aliquots of each serum containing 2×10^6 copies of HCV RNA were mixed and pooled serum sample with 1.2×10^7 copies was prepared as an inoculum. The pooled serum (2.5 mL) was added to the 3D cultured-FLC4 cells in the 30-mL RFB column, and the culture medium was changed after 12 h of incubation. At various times during the culture period, culture medium (50 mL) was collected to determine HCV RNA and the core protein. Collected culture media were passed through a 0.20-μm filter to remove the debris, and stored at −80 °C. In the second experiment to evaluate a therapeutic effect of anti-HCV drug (Fig. 4), 4-mL RFB columns were used. IFN-α (Sumiferon 300; Sumitomo Pharmaceuticals, Japan) was added to one of two columns at a final concentration of 100 IU/mL after the infection. Culture medium was periodically collected for determination of HCV RNA, the core protein and transaminases, and was replaced with the same volume of fresh medium with or without IFN-α.

2.3. Quantitation of HCV RNA and core protein

HCV RNA was extracted from 140 μL of each serum or culture medium using QIAamp Viral RNA Mini spin column (QIAGEN); RNA was eluted in 60 μL of water and stored at −80 °C. Real-time RT-PCR was performed using TaqMan EZ RT-PCR Core Reagents (PE Applied Biosystems), as described previously (Aizaki et al., 2003; Suzuki et al., 2005). The viral core antigen in the culture medium was quantified by immunoassay (Ortho HCV-Core ELISA Kit; Ortho-Clinical Diagnotics), according to the manufacturer's instruction (Murakami et al., 2006).

2.4. PCR amplification and nucleotide sequencing of HVR1 domain and its flanking region

Five microliters of RNA samples prepared as above were reverse transcribed using SuperScript II (Invitrogen) and a specific primer 5′-CATCCATGTGCAGCCGAACC-3′ (corresponding to nucleotides [nt] 2006–1987 of HCV NIHJ1) (Aizaki et al., 1998). For the nested PCR, a genotype-independent set of primers specific for hypervariable region 1 (HVR1). The first round of PCR was performed with the outer sense primer 5′-GCATGGCTTGGGATATGATG-3′ (nt 1291–1310) and with the reverse transcription primer described above as the outer antisense primer. After the initial 3.5-min denaturation step at 94 °C, 35 PCR cycles, with each cycle

Table 1
HCV-positive sera used in this study

Serum	Clone	HCV HVR1 sequence	% in the serum	genotype
A	A1	KVLIVMLSFAGVDGSTRTIGGRTAHTTQGSASLFSSGPAQKIQLINTNGS	75	1
	A2	-------L------N-H-V--AV-SS---FT---KL----------S---	12.5	
	A3	-------L------N-YAS---AGLL-R-V--I-TA----------S---	12.5	
B	B1	KVVVILLLAAGVDAGTNTIGGSAAQTTSGFTGLFRSGARQNIQLINTNGS	50	2
	B2	----------R	12.5	
	B3	----------S---------	12.5	
	B4	--L-V---F-----E-HVT--N-GR--A-LV--LTP--K----------	12.5	
	B5	--I----------	12.5	
C	C1	KVLIVMLLFAGVDGDTHVSGGTQGRAAYGLASLFALGPTQKIQLVNTNGS	83.3	1
	C2	----------A----------	16.7	
D	D1	KVLIVMLLFAGVDGVTHTSGAAAGHNARSLSGLFSLGSAQKLQLINTNGS	40	1
	D2	----------A-Y---GT--Y-TKTFT-F--R-PS--I--------	20	
	D3	----------T--Y---T-T----P--------V-----	10	
	D4	----------V---T----P--------V-----	10	
	D5	----------V-----	10	
	D6	----------Y-T--FT----S-----I--V-----	10	
E	E1	KVLIVMLLFAGVDGSTRVSGGQAGRVTKSLASFFSPGPQQKIQLVNSNGS	40	1
	E2	----------HGFT-L--A-S----------	30	
	E3	----------QGFT-L--A-S----------	10	
	E4	----------S-FT-L-TV----------	10	
	E5	----------N-Y---------AH--T-L--A-S----------	10	
F	F1	KVLIVMLLFAGVDGETNVMGGRAGHTTNTFTSLFSVGPAQKIQLVNSNGS	37	1
	F2	----------D-K----------S-L----N---S----------	27	
	F3	----------K----Q-----S-L----N---S----------	18	
	F4	----------A-------A--TK---------D----	9	
	F5	----------G---------A--A--L----TR--S----------	9	

consisting of 1 min at 94 °C, 2 min at 45 °C, and 3 min at 72 °C, were carried out, followed by a 10-min extension step at 72 °C. The second round was performed with the inner sense primer 5′-GGTAAGCTTTCCATGGTGGGGAACTGGGC-3′ (nt 1419–1447) and the inner antisense primer 5′-CTGGAATTCGCAGTCCTGTTGATGTGCCA-3′ (nt 1627–1599). The amplified products were cloned into the pGEM-T vector (Promega), and at least 8 independent clones were sequenced with an automatic DNA sequencer (ABI PRISM 310, PE Applied Biosystems).

3. Results

3.1. The outline of the RFB system

The RFB system was initially aimed at developing artificial liver tissues and allows liver-derived cells to maintain morphological appearance as well as their physiological functions, such as the ability to synthesize albumin and drug-metabolizing activity mediated by cytochrome P450 (Iwahori et al., 2003). Fig. 1 shows the outline of the RFB system. The bioreactor column consists of a vertically extended cylindrical matrix with porous glass microcarriers, which were most suitable for FLC4 culture as described in Section 2. The conditioning vessel is connected to a circulation system including tanks either for supplying fresh medium or for recovering sample aliquots. Oxygen consumption, temperature and pH of the culture medium are monitored continuously and conditioned in the vessel by computer and mass flow controller throughout the culture. Thus, the radial-flow configuration permits full contact between culture medium and cells at a physiologic perfusion flow rate, and prevents excessive shear stresses and a buildup of waste products, thus ensuring the long-term viability of 3D culture. For the long-term culture up to 110 days, temperature in the vessel gradually decreased from 37 to 30 °C as shown in Fig. 2A. The oxygen consumption, which indicates the cell growth condition, increased slowly from days 0 to 80 post-inoculation of the cells, and maintained a constant level afterwards. Under this condition, the production rate of albumin was found to be stable from days 15 to 105. The following experiments of HCV infection were done in such a stable phase of the cell condition after 3 weeks of pre-culture. Cell grown in the RFB column reached confluence at the end of culture (day 110) since the cells were observed outside the matrix bed (Fig. 2B).

3.2. Infection of HCV-positive sera to RFB cultured FLC4 cells

Previously, HCV RNA could be detected in FLC4 cells grown in the RFB up to 4 weeks of culture following inoculation with an HCV carrier plasmid (Aizaki et al., 2003). Establishment of a long-term stable culture system of human liver-derived cells

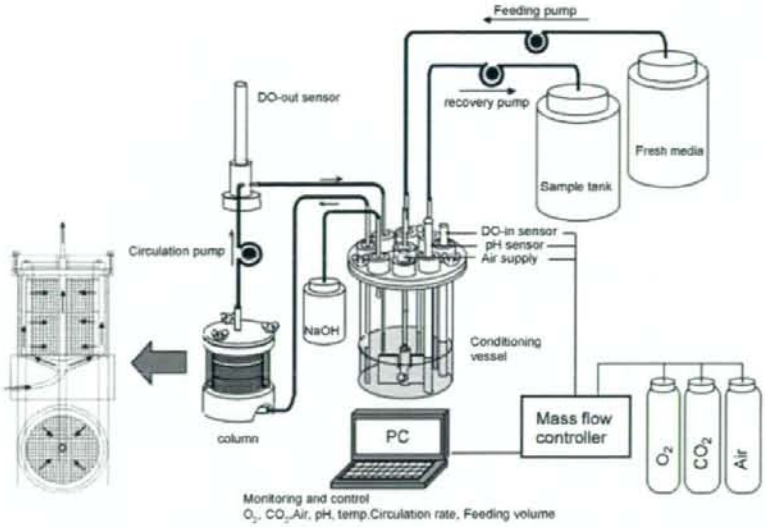

Fig. 1. Outline of the RFB system. RFB system consists of vessel, column and PC monitoring system. Culture condition was automatically controlled: oxgen concentration, temperature, pH, and oxgen level in the conditioning vessel are continuously monitored by PC and conditioned by mass flow controller.

retaining their differentiated hepatocyte function, as described above, enables evaluations of dynamic analysis of HCV replication and selection of viral variability and quasispecies. The potential of this culture system for screening HCV-positive sera was well suited for the viral infection.

Table 1 shows the serum samples (A–F) from six HCV carriers. The nucleotide complexity of HCV in serum samples was determined by sequencing the 1449–1598 nt region of the HCV genome, which includes HVR1 located at the N-terminal region of E2. Each serum was a mixture of a dominant HCV clone and related but distinct viral populations. The dominant species in sera A, C, D, E, and F were found to be genotype 1, and that in serum B was genotype 2. Viral loads in A–F, respectively, were 2.4×10^6, 8.6×10^6, 5.9×10^6, 2.5×10^6, 1.0×10^7 and 1.4×10^7 copies/mL, which were determined by real-time RT-PCR, as previously described (Aizaki et al., 2003; Suzuki et al., 2005). HCV loads of 2×10^6 copies from each serum sample were mixed to prepare a pooled serum sample containing 1.2×10^7 copies of HCV RNA. After FLC4 cells were inoculated into the RFB and subjected to 2 weeks of pre-culture for the preparation of 3D culture, the cells were infected with the pooled serum. Cell number at infection was about 10^8 in the 30-

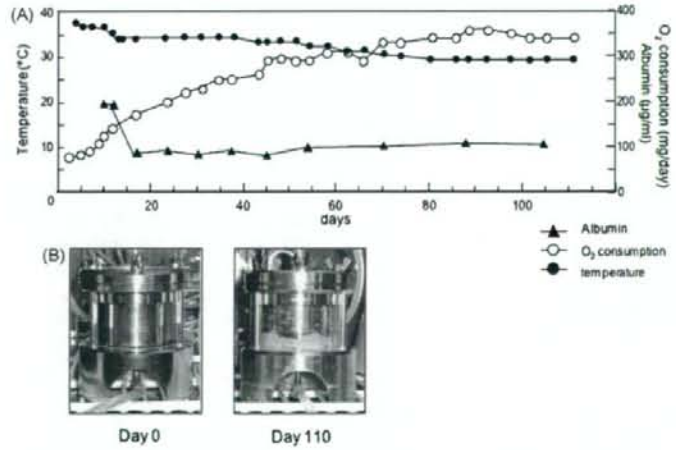

Fig. 2. Long-term culture of FLC4 cells in the RFB system. (A) Long-term culture of FLC4 cells in the RFB system. Temperature (closed circles) was gradually decreased from 37 to 30 °C. Oxygen consumption (open circles) was gradually increased from days 0 to 80 and reached the steady-state level. Albumin concentration (closed triangles) was constant from days 15 to 105. (B) The appearance of the RFB column at the beginning (day 0) and at the end (day 110) of culture.

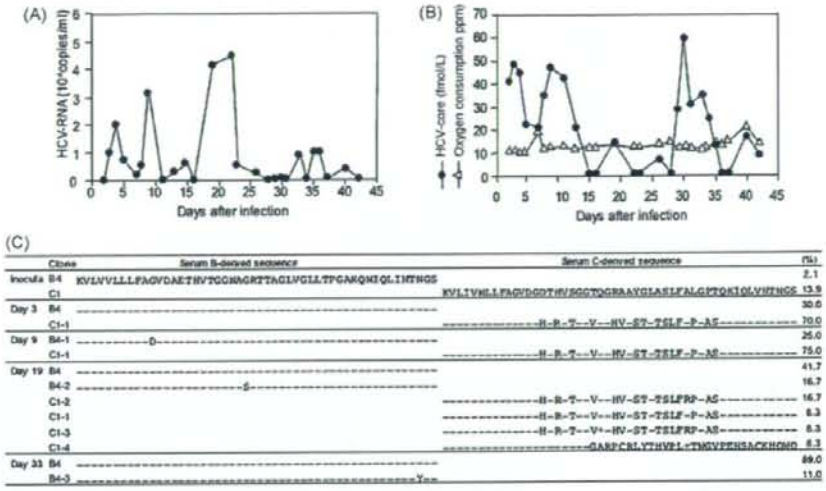

Fig. 3. HCV propagation in FLC4 cells cultured in the RFB system following inoculation with pooled sera obtained from HCV carriers. The 3D-cultured FLC4 cells were incubated with a pooled serum sample for 12 h, followed by changing the culture medium to fresh one. Culture medium was periodically collected for 42 days after inoculation, and HCV RNA and the viral core protein were quantified, respectively, by real-time RT-PCR and ELISA. (A) HCV RNA level in culture supernatant. (B) HCV-core protein (closed circles) and oxygen consumption (open triangles) levels in culture supernatant. (C) Changes in the viral quasispecies distribution after the inoculation. Percentages in the inoculum or in the culture medium at each time point (day 3, 9, 19, or 33 p.i.) are indicated at the right side. *, termination codon.

mL RFB column, as estimated from the glucose consumption (Kawada et al., 1998). Culture medium in the RFB was replaced with fresh medium 12 h post-infection (p.i.) and periodically sampled for 42 days.

Fig. 3A and B shows the levels of HCV RNA and viral core protein in the culture medium, respectively. HCV RNA was not observed on the first 2 days following infection, but was detectable from day 3 p.i. Viral RNA levels fluctuated, with peaks on days 3, 9, 19–21 and 33–36 p.i. At days 19–21 p.i., the average amount of HCV RNA detected in the culture supernatant was approximately 3×10^6 copies/day. Intermittent peaks were observed in HCV core protein levels in the culture supernatant, and the peak pattern of the core protein was largely consistent with that of viral RNA. During the infection experiment, the level of oxygen consumption was constant at approximately 12 ppm, thus suggesting that the desired conditions (constant or very gradually increasing cell number) were maintained.

3.3. Quasispecies analysis in RFB culture

The above results suggest that, although the environment was consistent in the pooled serum infection, there were periods in which the viruses actively replicated and released from the cells and periods in which they poorly replicated. The pooled serum used for the infection exhibited HCV populations had at least 26 distinct quasispecies (Table 1). To investigate whether the quasispecies distribution was altered due to infection, and whether HCV populations are selected during long-term culture in the RFB, total RNA was extracted from the culture supernatant samples collected on days 3, 9, 19 and 33 p.i., and the nucleotide sequence of the region containing HVR1 was determined, as described above. As shown in Fig. 3C, it is of interest that only two HCV species were detected in the sample at day 3 p.i.; the dominant clone C1-1, comprising approximately 70% of the viral population, and clone B4, comprising 30%. Although clone C1-1 was not detected in the sequence of the inoculum shown in Table 1, it was most similar to clone C1, a dominant clone in plasma C, among the HCV population observed in the inoculum; thus, it is possible that clone C1-1 is one of the minor species in serum C. Clone B4 was found to be derived from serum B. An almost identical HCV population was observed in the sample at day 9 p.i. In this sample, the dominant clone C1-1 and clone B4-1, which differs from clone B4 by only one amino acid, were detected. In contrast, more significant variation in quasispecies structure of the HCV species was observed in the sample at day 19 p.i. than that at day 9 p.i. With B4 as the dominant clone, the serum B-derived HCV species, clones B4 and B4-2, which differs from clone B4 by one amino acid, comprised 58% of the total population. Four types of HCV sequences derived from serum C were detected. Two of these (clones C1-3 and C1-4) contained lethal mutations. It was also found that the HCV species detected in the sample at day 33 p.i. included only two clones (clones B4 and B4-3), derived from serum B. The dominant clone, B4, was found to comprise 89% of the total population.

3.4. Potential use of the RFB system for evaluation of anti-HCV compounds

An experiment was carried out to determine whether this HCV infection experiment system was useful for the evaluation of anti-HCV drugs (Fig. 4). For this purpose, a small,

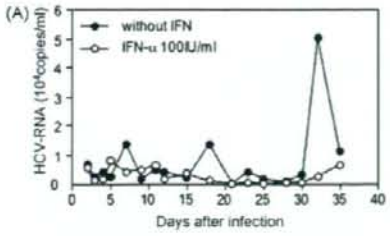

(B)

	Clone		(%)
Inocula	B4	KYLYYLLLFAGYDAETKTTGGNAGRTTAGLVGLLTPGAKQNIQLINTNGS	2.1
	C1	KYLIYVLLFAGYDGDTKTSGGTQGRAATGLASLFALGFTQKIQLVNTNGS	13.9
Day 32	B4	----------	60
	B4-4	----------*----------	20
	C1-1	----------H-R-T--T--NT-ST-TSLF-P-AS----------	20

Fig. 4. A therapeutic effect of IFN in HCV infection model in the RFB cultures. HCV-infected FLC4 cells were treated with or without 100 IU/mL IFN-α. (A) Culture media were periodically collected, and HCV RNA levels were determined. Closed circles: without IFN treatment, open circles: treatment with IFN. (B) Changes in the viral quasispecies distribution in the cells without IFN treatment. Percentages in the inoculum or in the culture medium on day 32 p.i. are indicated at the right side. *, termination codon.

4-mL RFB column was adopted and a pair of RFB cultures infected with the HCV-positive pooled plasma (Table 1) was prepared. IFN-α was added to one culture at a final concentration of 100 IU/mL at 12 h p.i. No cytotoxicity was observed in FLC4 cells under these conditions (data not shown). Culture media from two cultures (12.5 mL each) were sampled periodically for 35 days and replaced by the same volume of fresh medium in the presence or absence of IFN-α. HCV RNA in the collected media was quantified by real-time RT-PCR, as described above. As shown in Fig. 4A, in the no-treatment culture, fluctuations in the viral RNA levels with the peaks on days 7, 18, and 32 p.i. ($1.5–5 \times 10^4$ copies/mL) were observed. However, while HCV RNA at $0.5–0.8 \times 10^4$ copies/mL was detected in the IFN-treated culture at days 5–11 p.i., no HCV RNA was detected at days 12–30 p.i. Serum levels of hepatic transaminases such as ALT and AST are known to be markers of liver damage. In the HCV-infection model with FLC4 cells cultured in RFB, the AST levels in the culture medium, which ranged from 5 to 10 IU/L without HCV infection, increased to 20–50 IU/L according to the viral infection (data not shown). Such increased AST levels were found to fall by the IFN treatment to lower than 10 IU/L at day 28 p.i. As reported previously, the ALT levels in the culture medium were constantly low; its levels were less than 10 IU/mL, with or without HCV infection (Aizaki et al., 2003). The viral nucleotide sequence in the no-treatment culture medium at day 32 p.i. was determined. It was found that serum B-derived clone B4 was dominant, and serum C-derived clone C1 was present as a minor clone (Fig. 4B); thus, the results corresponded well with those demonstrated in Fig. 3. An increase in viral RNA in the IFN-treated culture after day 32 p.i. was observed; although the degree of increase was only slight (Fig. 4A). It will be interesting to test whether HCV species grown in the IFN-treated culture is a variant resistant to IFN-α.

4. Discussion

At present an important limitation of the *in vitro* HCV infection system is that the only established culture system is based on genotype 2a, JFH-1 isolate, and Huh-7-derived cell lines. The development of alternate infection systems in which other HCV strains and host cells are available has been needed for the study of HCV dynamics and virus–host interactions, and for testing antivirals. This paper demonstrates that a long-term culture of the 3D RFB system is a useful tool for investigating HCV dynamics. The present results revealed that the viral quasispecies distribution altered in the HCV infection system in the RFB system. The change probably occurs in the following two-stage process. The first change was observed on day 3 p.i.; thus, it is possible that the HCV species were selected according to infectivity in FLC4 cells. It has been reported that HCV particle populations in chronic hepatitis C patients consist of low-density virions and higher-density immune complex forms (Hijikata et al., 1993; Kanto et al., 1994). Inoculation of cultured cells with HCV has demonstrated that the immune complex forms were less infective than the antibody-unbound virions (Shimizu et al., 1994). Therefore, another hypothesis may be that a large number of HCV populations in sera A, D, E, and F are immune complex forms; thus, these sera are less susceptible to the cells than sera B and C. The second change was observed on days 19–33 p.i. While the serum C-derived clone was dominant in the early stages after infection, the serum B-derived HCV clone became dominant over time. In the absence of immunological selection pressure, viral nucleotide mutations at random positions are accumulated during viral replication, and the newly generated variant species are selected principally, if not solely, based on the intrinsic replicative advantages or disadvantages that these mutations confer. Thus, these results suggest that the use of pooled serum sample allowed for screening of infectious materials compatible for the RFB culture.

Evaluation methods for anti-HCV drugs using monolayer culture systems with various culture cells, such as the replicon system and the JFH-1 based virion production system, have been reported (Bartenschlager et al., 2003; Blight et al., 2000; Boriskin et al., 2006; Lanford et al., 2003; Lindenbach et al., 2005; Lohmann et al., 1999; Wakita et al., 2005; Zhong et al., 2005). These methods utilize viral markers, such as HCV RNA and antigens, as indicators of treatment efficacy. However, the utility of long-term cell culture systems for anti-HCV drug evaluation based on infection with human sera is still limited. The use of a chimpanzee model, the only non-human host for HCV infection, is restricted due to several reasons such as problematic availability and ethical consideration. Given intensive efforts to reduce and replace animal testing in the course of development of new therapies worldwide, the RFB-based HCV infection model is a potential alternative to animal models such chimpanzee for assessing anti-HCV compounds. According to the studies with regards to mathematical modeling of HCV kinetics (Dahari et al., 2005; Dixit et al., 2004; Layden et al., 2003; Layden-Almer et al., 2006; Perelson et al., 2005), IFN therapy against HCV infection generally generates a biphasic decline in viral load; there is a rapid decrease in the serum HCV RNA level over the

first 1 day of treatment, followed by the second phase, which is slower than the first-phase viral decline. To date, there were no such observable viral kinetics in the IFN treatment under such experimental settings. Further detailed kinetic analyses of the use of varying doses of IFN and of very early time points to evaluate the antiviral effect are in progress.

In summary, by investigating the dynamics of HCV populations in the RFB culture system, it was demonstrated that HCV was intermittently detected in the culture supernatants of long-term culture, and that changes in viral quasispecies appear to be related to this fluctuation in the virus level. It was also shown that an HCV-infection model using the RFB system is useful for evaluating potential antivirals. Further investigation on the infection and growth of various HCV-positive sera is currently being conducted in order to obtain an adaptive clone with higher replication efficiency in this culture system.

Acknowledgements

The authors thank T. Wakita and S. Nagamori for helpful discussion and suggestions. We also thank M. Matsuda, T. Shimoji and M. Yahata for technical assistance, and T. Mizoguchi for secretarial work. This work was supported in part by a grant for Research on Health Sciences focusing on Drug Innovation from the Japan Health Sciences Foundation; by grants-in-aid from the Ministry of Health, Labor and Welfare; and by the program for Promotion of Fundamental Studies in Health Sciences of the National Institute of Biomedical Innovation, Japan.

References

Aizaki, H., Aoki, Y., Harada, T., Ishii, K., Suzuki, T., Nagamori, S., Toda, G., Matsuura, Y., Miyamura, T., 1998. Full-length complementary DNA of hepatitis C virus genome from an infectious blood sample. Hepatology 27, 621–627.

Aizaki, H., Nagamori, S., Matsuda, M., Kawakami, H., Hashimoto, O., Ishiko, H., Kawada, M., Matsuura, T., Hasumura, S., Matsuura, Y., Suzuki, T., Miyamura, T., 2003. Production and release of infectious hepatitis C virus from human liver cell cultures in the three-dimensional radial-flow bioreactor. Virology 314, 16–25.

Aoki, Y., Aizaki, H., Shimoike, T., Tani, H., Ishii, K., Saito, I., Matsuura, Y., Miyamura, T., 1998. A human liver cell line exhibits efficient translation of HCV RNAs produced by a recombinant adenovirus expressing T7 RNA polymerase. Virology 250, 140–150.

Bartenschlager, R., Kaul, A., Sparacio, S., 2003. Replication of the hepatitis C virus in cell culture. Antivir. Res. 60, 91–102.

Blight, K.J., Kolykhalov, A.A., Rice, C.M., 2000. Efficient initiation of HCV RNA replication in cell culture. Science 290, 1972–1974.

Boriskin, Y.S., Pecheur, E.I., Polyak, S.J., 2006. Arbidol: a broad-spectrum antiviral that inhibits acute and chronic HCV infection. Virol. J. 3, 56.

Choo, Q.L., Kuo, G., Weiner, A.J., Overby, L.R., Bradley, D.W., Houghton, M., 1989. Isolation of a cDNA clone derived from a blood-borne non-A, non-B viral hepatitis genome. Science 244, 359–362.

Choo, Q.L., Richman, K.H., Han, J.H., Berger, K., Lee, C., Dong, C., Gallegos, C., Coit, D., Medina-Selby, R., Barr, P.J., et al., 1991. Genetic organization and diversity of the hepatitis C virus. Proc. Natl. Acad. Sci. U.S.A. 88, 2451–2455.

Dahari, H., Major, M., Zhang, X., Mihalik, K., Rice, C.M., Perelson, A.S., Feinstone, S.M., Neumann, A.U., 2005. Mathematical modeling of primary hepatitis C infection: noncytolytic clearance and early blockage of virion production. Gastroenterology 128, 1056–1066.

Dixit, N.M., Layden-Almer, J.E., Layden, T.J., Perelson, A.S., 2004. Modelling how ribavirin improves interferon response rates in hepatitis C virus infection. Nature 432, 922–924.

Grakoui, A., McCourt, D.W., Wychowski, C., Feinstone, S.M., Rice, C.M., 1993. Characterization of the hepatitis C virus-encoded serine proteinase: determination of proteinase-dependent polyprotein cleavage sites. J. Virol. 67, 2832–2843.

Hijikata, M., Kato, N., Ootsuyama, Y., Nakagawa, M., Shimotohno, K., 1991. Gene mapping of the putative structural region of the hepatitis C virus genome by in vitro processing analysis. Proc. Natl. Acad. Sci. U.S.A. 88, 5547–5551.

Hijikata, M., Shimizu, Y.K., Kato, H., Iwamoto, A., Shih, J.W., Alter, H.J., Purcell, R.H., Yoshikura, H., 1993. Equilibrium centrifugation studies of hepatitis C virus: evidence for circulating immune complexes. J. Virol. 67, 1953–1958.

Hongo, T., Kajikawa, M., Ishida, S., Ozawa, S., Ohno, Y., Sawada, J., Umezawa, A., Ishikawa, Y., Kobayashi, T., Honda, H., 2005. Three-dimensional high-density culture of HepG2 cells in a 5-ml radial-flow bioreactor for construction of artificial liver. J. Biosci. Bioeng. 99, 237–244.

Ikeda, M., Sugiyama, K., Mizutani, T., Tanaka, T., Tanaka, K., Sekihara, H., Shimotohno, K., Kato, N., 1998. Human hepatocyte clonal cell lines that support persistent replication of hepatitis C virus. Virus Res. 56, 157–167.

Iwahori, T., Matsuura, T., Maehashi, H., Sugo, K., Saito, M., Hosokawa, M., Chiba, K., Masaki, T., Aizaki, H., Ohkawa, K., Suzuki, T., 2003. CYP3A4 inducible model for in vitro analysis of human drug metabolism using a bioartificial liver. Hepatology 37, 665–673.

Kanto, T., Hayashi, N., Takehara, T., Hagiwara, H., Mita, E., Naito, M., Kasahara, A., Fusamoto, H., Kamada, T., 1994. Buoyant density of hepatitis C virus recovered from infected hosts: two different features in sucrose equilibrium density-gradient centrifugation related to degree of liver inflammation. Hepatology 19, 296–302.

Kawada, M., Nagamori, S., Aizaki, H., Fukaya, K., Niiya, M., Matsuura, T., Sujino, H., Hasumura, S., Yashida, H., Mizutani, S., Ikenaga, H., 1998. Massive culture of human liver cancer cells in a newly developed radial flow bioreactor system: ultrafine structure of functionally enhanced hepatocarcinoma cell lines. In Vitro Cell Dev. Biol. Anim. 34, 109–115.

Kuo, G., Choo, Q.L., Alter, H.J., Gitnick, G.L., Redeker, A.G., Purcell, R.H., Miyamura, T., Dienstag, J.L., Alter, M.J., Stevens, C.E., et al., 1989. An assay for circulating antibodies to a major etiologic virus of human non-A, non-B hepatitis. Science 244, 362–364.

Lanford, R.E., Guerra, B., Lee, H., Averett, D.R., Pfeiffer, B., Chavez, D., Notvall, L., Bigger, C., 2003. Antiviral effect and virus-host interactions in response to alpha interferon, gamma interferon, poly(i)–poly(c), tumor necrosis factor alpha, and ribavirin in hepatitis C virus subgenomic replicons. J. Virol. 77, 1092–1104.

Layden, T.J., Layden, J.E., Ribeiro, R.M., Perelson, A.S., 2003. Mathematical modeling of viral kinetics: a tool to understand and optimize therapy. Clin. Liver Dis. 7, 163–178.

Layden-Almer, J.E., Cotler, S.J., Layden, T.J., 2006. Viral kinetics in the treatment of chronic hepatitis C. J. Viral Hepat. 13, 499–504.

Lindenbach, B.D., Evans, M.J., Syder, A.J., Wolk, B., Tellinghuisen, T.L., Liu, C.C., Maruyama, T., Hynes, R.O., Burton, D.R., McKeating, J.A., Rice, C.M., 2005. Complete replication of hepatitis C virus in cell culture. Science 309, 623–626.

Lohmann, V., Korner, F., Koch, J., Herian, U., Theilmann, L., Bartenschlager, R., 1999. Replication of subgenomic hepatitis C virus RNAs in a hepatoma cell line. Science 285, 110–113.

Martell, M., Esteban, J.I., Quer, J., Genesca, J., Weiner, A., Esteban, R., Guardia, J., Gomez, J., 1992. Hepatitis C virus (HCV) circulates as a population of different but closely related genomes: quasispecies nature of HCV genome distribution. J. Virol. 66, 3225–3229.

Murakami, K., Ishii, K., Ishihara, Y., Yoshizaki, S., Tanaka, K., Gotoh, Y., Aizaki, H., Kohara, M., Yoshioka, H., Mori, Y., Manabe, N., Shoji, I., Sata, T., Bartenschlager, R., Matsuura, Y., Miyamura, T., Suzuki, T., 2006. Production of infectious hepatitis C virus particles in three-dimensional cultures of the cell line carrying the genome-length dicistronic viral RNA of genotype 1b. Virology 351, 381–392.